LUND UNIVERSITY

Characteristics of fresh and aged carbonaceous aerosol from anthropogenic combustion sources

Nordin, Erik

2015

Characteristics of fresh and aged carbonaceous aerosol from anthropogenic combustion sources

Erik Nordin

LUND
UNIVERSITY

DOCTORAL DISSERTATION
by due permission of the Faculty of Technology, Lund University, Sweden.

To be defended at Stora hörsalen, IKDC, Lund. 2015-01-30 10:15.

Faculty opponent

Associate Professor Annele Virtanen, Department of Applied Physics,
University of Eastern Finland, Kuopio, Finland

Organization	Document name
LUND UNIVERSITY	Doctoral Thesis
Department of Design Sciences	Date of issue
Division of Ergonomics and Aerosol Technology	2015-01-07
Author(s) Erik Nordin	Sponsoring organization

Title and subtitle

Characteristics of fresh and aged carbonaceous aerosol from anthropogenic combustion sources

Abstract

Emissions from anthropogenic combustion sources, such as light duty vehicles and small scale biomass combustion, contribute significantly to ambient aerosol particle concentrations both on local and global scales. These emissions have controlling impacts on public health and global climate. The overall aim of this thesis was to investigate how atmospheric transformation and combustion conditions affect the health and climate relevant characteristics of anthropogenic combustion aerosol.

The formation of secondary organic aerosol (SOA) from photo-oxidized gasoline vehicle exhaust was studied in a smog chamber. The physical and chemical properties of particulate emissions from small scale biomass combustion were investigated as a function of burn rate with on-line instrumentation including differential mobility analyzer-aerosol particle mass analysis (DMA-APM) and aerosol mass spectrometry (AMS). Samples of fresh and aged biomass combustion aerosol were collected to investigate the toxicological properties. Finally, the mass-mobility relationship and mixing state of urban aerosol were investigated with the DMA-APM technique.

SOA production clearly dominated over primary organic emissions for gasoline vehicle exhaust, opposite to diesel exhaust. Up to 60% of the SOA formed from gasoline vehicle exhaust originated from traditional light aromatic SOA precursors, significantly higher than previous data for diesel exhaust.

Particulate phase polycyclic aromatic hydrocarbons (PAHs) were quantified with high time resolution during different phases of the combustion cycle. PAH emissions were a factor seven higher for high burn rate compared to nominal operation of the wood stove. The majority of PAHs was emitted during the intermediate (flaming) phase of the combustion.

Three main types of biomass combustion particles were found: spherical organic aerosol, soot agglomerates and compact inorganic ash particles. The combustion conditions affected the mass mobility relationship of the aerosol from full combustion cycles.

Effects on cell viability were strongest for less efficient combustion (high PAHs and OA fraction). The genotoxic response increased upon dark aging with ozone, possibly due to PAH degradation products.

The particles observed during the urban campaign could be divided into two groups according to their mass-mobility relationship, soot (less compact) and long-range transport particles (more compact). The long-range transport particles were to a higher extent present during days of polluted easterly winds. The soot particles in urban air had similar properties as soot particles emitted from diesel engines in laboratory studies.

The results presented in this thesis show that the physical, chemical and toxicological properties of carbonaceous aerosol from combustion are affected by source, combustion conditions and atmospheric aging. This needs to be taken into account when assessing health and climate effects of aerosol particles.

Key words: Aerosol, biomass combustion, gasoline vehicle exhaust, polycyclic aromatic hydrocarbons, secondary organic aerosol, soot, mass-mobility relationship, emissions, toxicity

Classification system and/or index terms (if any)

Supplementary bibliographical information | Language: English

ISSN and key title: 1650-9773 Publication 53 (EAT 2015) | ISBN:978-91-7623-223-1

Recipient's notes | Number of pages 148 | Price

Security classification

Characteristics of fresh and aged carbonaceous aerosol from anthropogenic combustion sources

Erik Nordin

LUND
UNIVERSITY

Cover picture by Kirsten I. Kling

Faculty of Engineering, Department of Design Sciences
ISBN 978-91-7623-223-1 (Printed)
ISBN 978-91-7623-224-8 (Pdf)
ISSN 1650-9773 Publication 53

Printed in Sweden by Media-Tryck, Lund University
Lund 2015

Contents

Appended papers

I) **Nordin, E. Z.**, Eriksson, A. C., Roldin, P., Nilsson, P. T., Carlsson, J. E., Kajos, M. K., Hellén, H., Wittbom, C., Rissler, J., Löndahl, J., Swietlicki, E., Svenningsson, B., Bohgard, M., Kulmala, M., Hallquist, M., and Pagels, J. H. (2013) Secondary organic aerosol formation from idling gasoline passenger vehicle emissions investigated in a smog chamber, Atmos Chem Phys, 13, 6101-6116, doi:10.5194/acp-13-6101-2013

II) Eriksson, A. C., **Nordin, E. Z.**, Nyström, R., Pettersson, E., Swietlicki, E., Bergvall, C., Westerholm, R., Boman, C. and Pagels, J. H. (2014). Particulate PAH emissions from residential biomass combustion: time-resolved analysis with aerosol mass spectrometry. Environ Sci Technol 48(12): 7143-7150.

III) **Nordin, E. Z.**, Eriksson, A. C., Nyström, R., Lindgren, R., Nielsen, I. E., Kling, K. I., Berg-Malmborg, V., Rissler, J., Boman, C., and Pagels, J. H. Mass-mobility relationship and mixing state of aerosol from small-scale biomass combustion. Manuscript in preparation

IV) **Nordin, E. Z.,** Uski, O., Nyström, R., Jalava, P., Eriksson, A. C., Genberg, J., Roldin, P., Bergvall, C., Westerholm, R., Jokiniemi, J., Pagels, J. H., Boman, C. and Hirvonen, M.-R. (2015). Influence of ozone initiated processing on the toxicity of aerosol particles from small scale wood combustion. Atmos Environ 102(0): 282-289.

V) Rissler, J., **Nordin, E. Z.**, Eriksson, A. C., Nilsson, P. T., Frosch, M., Sporre, M. K., Wierzbicka, A., Svenningsson, B., Löndahl, J., Messing, M. E., Sjögren, S., Hemmingsen, J. G., Loft, S., Pagels, J. H. and Swietlicki, E. (2014). Effective density and mixing state of aerosol particles in a near-traffic urban environment. Environ Sci Technol 48(11): 6300-6308.

The authors' contributions to the papers

I) I had a major role in planning and performing the experiments, and in designing and implementing the measurement setup. I analyzed parts of the data and wrote most of the paper.

II) I participated in planning and performing the experimental work. I was involved in analyzing the experimental data and I wrote parts of the paper.

III) I had a major role in planning and performing the experiments. I analyzed the majority of the data and I wrote the paper.

IV) I had a major role in planning and executing the experimental work of collecting fresh and aged aerosol. I analyzed the data from the on-line aerosol instruments. I wrote major parts of the paper.

V) I participated in planning and execution of the measurement campaign. I analyzed the DMA-APM data. I wrote parts of the paper.

Related publications (not included in this thesis)

Peer reviewed papers

Rissler, J., Messing, M. E., Malik, A. I., Nilsson, P. T., **Nordin, E. Z.**, Bohgard, M., Sanati, M. and Pagels, J. H. (2013). Effective density characterization of soot agglomerates from various sources and comparison to aggregation theory. Aerosol Sci Tech 47(7): 792-805.

Isaxon, C., Gudmundsson, A., **Nordin, E.Z.**, Lönnblad, L., Dahl, A., Wieslander, G., Bohgard, M. and Wierzbicka, A. (2014). Contribution of indoor-generated particles to residential exposure. Atmos Environ., in press. Available on-line doi:10.1016/j.atmosenv.2014.07.053

Roldin, P., Eriksson, A. C., **Nordin, E. Z.**, Hermansson, E., Mogensen, D., Rusanen, A., Boy, M., Swietlicki, E., Svenningsson, B., Zelenyuk, A. and Pagels, J. (2014) Modelling non-equilibrium secondary organic aerosol formation and evaporation with the aerosol dynamics, gas- and particle-phase chemistry kinetic multilayer model ADCHAM, Atmos Chem Phys, 14, 7953-7993, doi:10.5194/acp-14-7953-2014

Wittbom, C., Eriksson, A. C., Rissler, J., Carlsson, J. E., Roldin, P., **Nordin, E. Z.**, Nilsson, P. T., Swietlicki, E., Pagels, J. H. and Svenningsson, B. (2014) Cloud droplet activity changes of soot aerosol upon smog chamber ageing, Atmos. Chem. Phys., 14, 9831-9854, doi:10.5194/acp-14-9831-2014

Conference proceedings (selection)

Nordin, E. Z., Lindskog, M., Nilsson, P., Rissler, J., Swietlicki, E., Bohgard, M. and Pagels J. *Lund University Smog Chamber*. Nordic Society for Aerosol Research (NOSA) Conference, Lund, Sweden, 2009.

Nordin, E. Z., Nilsson, P., Eriksson, A., Kajos, M.K., Rissler, J., Svenningsson, B., Swietlicki, E., Bohgard, M., Kulmala, M., and Pagels, J. *Chamber studies of secondary aerosol formation from light duty vehicle exhausts*. International Aerosol Conference (IAC), Helsinki, Finland, 2010.

Nordin, E. Z., Eriksson, A.C., Carlsson, J.E., Nilsson, P., Kajos, M.K., Roldin, P., Rissler, J., Swietlicki, E., Svenningsson, B., Bohgard, M., Kulmala, M., Hallquist., M. and Pagels, J. *Smog Chamber Studies on SOA Formation from Gasoline Exhaust and Pure Precursors.* European Aerosol Conference (EAC) Manchester, UK, 2011.

Nordin, E. Z., Pagels, J., Eriksson, A., Nyström, R., Pettersson, E., Swietlicki, E., Bohgard, M. and Boman, C. *On-line Characterization of Biomass Aerosols from Different Combustion Conditions.* European Aerosol Conference (EAC) Manchester, UK, 2011.

Pagels, J., Eriksson, A., **Nordin, E. Z.**, Nyström, R., Pettersson, E. and Boman, C. *Time resolved PAH-emissions from residential wood combustion*. European Aerosol Conference (EAC) Manchester, UK, 2011.

Nordin, E. Z., Eriksson, A., Nyström, R., Pettersson, E., Rissler, J., Swietlicki, E., Bohgard, M.,Boman, C. and Pagels, J. *On-line Characterization of Aerosols from Transient Biomass Combustion*. European Aerosol Conference (EAC) Granada, Spain, 2012.

Rissler, J., Nilsson, P.T., Pagels, J., Eriksson, A. C., **Nordin, E.Z.**, Swietlicki, E., Svenningsson, B., Frosch, M., Ahlberg, E., Wittbom, C., Löndahl, J., Wierzbicka, A., Hemmingsen, J.G.. Loft, S. and Sjögren, S. *Effective density of particles in an urban environment – measured with a DMA-APM system for lung dose estimations.* European Aerosol Conference (EAC) Granada, Spain, 2012.

Eriksson, A., **Nordin, E.Z.**, Nyström R., Pettersson, E., Bergwall, C., Westerholm, R., Swietlicki, E., Boman C. and Pagels J. *Polycyclic Aromatic Hydrocarbon Emissions from Transient Wood Combustion.* American Association for Aerosol Research (AAAR) Annual Conference, Minneapolis, USA, 2012

Nordin, E.Z., Uski, O., Nyström, R., Jalava, P., Genberg, J., Eriksson, A.C., Bergvall, C., Westerholm R., Boman, C., Jokiniemi, J., Pagels, J. and Hirvonen, M-R. T*oxicological Responses to Ozone Aging of Aerosols from Small-scale Biomass Combustion.* European Aerosol Conference (EAC) Prague, Czech Republic, 2013

Pagels, J.H. Eriksson, A.C., Rissler, J., **Nordin, E.Z.**, Wittbom, C., Nilsson, P.T., Roldin, P., Svenningsson B. and Swietlicki E. T*ransformation of Black Carbon Aerosol in the Atmosphere –Observations from Smog Chamber Studies and Ambient Air.* European Aerosol Conference (EAC) Prague, Czech Republic, 2013

Nordin E. Z., Rissler J., Eriksson A.C., Hermansson E., Kristensson A., Swietlicki E. and Pagels J. *Mass-mobility measurements of urban and background aerosol – measured with a DMA-TD-APM system.* American Association for Aerosol Research (AAAR) Annual Conference, Portland, USA, 2013

Rissler, J., **Nordin, E.Z.**, Eriksson, A.C., Messing, M.E.,. Nilsson, P.T., Svenningsson, B. Frosch, M., Wierzbicka, A., Hemmingsen, J.G., Loft, S., Sjögren, S., Pagels, J. and Swietlicki E. *On-line measurements of soot aggregates in a near-traffic urban environment – with applications to surface area and lung dose estimations.* Gesellschaft fûr Aerosolforschung e.V. (GAeF) Aerosol technology Conference, Karlsruhe, Germany, 2014

Nordin, E. Z., Eriksson, A.C., Nyström, R., Lindgren, R., Rissler, J., Boman, C. and Pagels, J.H. *Mixing state and mass mobility relationship of aerosol from small scale biomass combustion.* International Aerosol Conference (IAC), Busan, South Korea, 2014

Eriksson, A.C., **Nordin, E. Z.**, Nyström, R., Lindgren, R., Martinsson, J., Ahlberg, E., Svenningsson, B., Swietlicki, E., Boman, C. and Pagels, J.H. *Time-Resolved Biomass Combustion Emissions – Impacts of Burn Rate and Atmospheric Processing.* International Aerosol Conference (IAC), Busan, South Korea, 2014

Reports

Boman, C. et al., *Emissioner från småskalig värmeförsörjning med biobränsle*, Energimyndigheten Slutrapport Projekt P30824-1, ISSN 1653-0551 ETPC Report 11-05

Jokiniemi, J., Tissari, J. et al., *BIOHEALTH – Health effects of particulate emissions from small scale biomass combustion*, ERA-NET Bioenergy Program 6th Joint Call on Clean Biomass Combustion Final Report, 2013

Symbols and abbreviations

ε_m	Mass-mobility exponent
ρ_{eff}^{I}	Effective density from mass-mobility measurements
ρ_{eff}^{III}	Effective density from aerodynamic and mobility diameter measurements

AMS	Aerosol mass spectrometer/metry
APM	Aerosol particle mass analyzer
BC	Black carbon
BrC	Brown carbon
CPC	Condensation particle counter
DGI	Dekati gravimetric impactor
DMA	Differential mobility analyzer
d_m	Mobility (equivalent) diameter (Paper V)
d_{me}	Mobility (equivalent) diameter
d_{va}	Vacuum aerodynamic diameter
EC	Elemental carbon
ELVs	Emissions limit values, in regards to biomass combustion
GC-MS	Gas chromatography-mass spectrometry
HAS	Hot air starved (combustion)
HB	High burn rate
J_{NO_2}	NO_2 Photolysis rate
LA	Light aromatic organic compounds
m_{agg}	Aggregate mass
m/z	Mass to charge ratio

NB	Nominal burn rate – Paper II and III
NOM	Nominal burn rate – Paper IV
OA	Organic aerosol
OC	Organic carbon
PAHs	Polycyclic aromatic hydrocarbons
PM	Particulate matter
POA	Primary organic aerosol
PTR-MS	Proton transfer reaction – mass spectrometer
rBC	Refractory black carbon
SMPS	Scanning mobility particle sizer
SOA	Secondary organic aerosol
SP-AMS	Aerosol mass spectrometer equipped with a laser vaporizer
TD	Thermodenuder
V_{APM}	APM voltage
VBS	Volatility basis set
VOCs	Volatile organic compounds

Populärvetenskaplig sammanfattning

Luftburna partiklar från transportsektorn och energiproduktion kan ge upphov till negativa hälsoeffekter hos människor och påverka det globala klimatet. Partiklarnas kemiska och fysikaliska egenskaper förändras när de åldras i atmosfären och ny partikelmassa kan bildas från ämnen som tidigare var i gasfas. Det övergripande syftet med den här avhandlingen är att öka kunskapen om egenskaperna hos luftburna partiklar från förbränningskällor, för att på längre sikt öka förståelsen hur dessa partiklar påverkar människors hälsa och klimatet.

Våra experiment visar att det bildas ny sekundär partikelmassa av avgaserna från bensindrivna personbilar, som går på tomgång, när de utsätts för simulerad atmosfärisk åldring genom UV-ljus. Den nybildade partikelmassan är betydligt större än partikelmassan som emitteras primärt från avgasröret. Trots detta finns det idag endast emissionsbegränsningar för primära partikelemissioner men inte för sekundärt bildad partikelmassa.

Idag finns det rekommendationer kring vedeldning som säger att man ska använda ”lagom torr ved” eftersom fuktig ved ger ökade utsläpp av luftföroreningar. Resultat i den här avhandlingen visar att försnabb förbränning ger upphov till förhöjda utsläpp av polycykliska aromatiska kolväten (PAHer) och de förhöjda utsläppen av PAHer sammanfaller med låg syrehalt i rökgaserna. PAH-utsläpp är något som bör undvikas då det finns misstankar att PAHer kan vara cancerframkallande och därför bör även snabb syrefattig förbränning undvikas.

Som tidigare nämnts så kan luftburna partiklars kemiska och fysikaliska egenskaper förändras i atmosfären och det finns därför skäl att tro att dessa förändringar påverkar tocixiteten hos partiklarna. För att öka förståelsen hur toxiciteten hos vedrökspartiklar förändras vid atmosfärisk åldring samlades färska och åldrade partikelprover in. De insamlade partiklarna användes för att exponera celler, som sedan genomgick flera olika toxikologiska tester. Resultaten, för några av de toxikologiska testerna visade på en skillnad i respons från de celler som exponerats för de åldrade partiklarna jämfört med de som exponerats för de icke-åldrade partiklarna. Detta visar att man bör ta hänsyn till effekten av åldring när man bedömer hälsoeffekter från vedrök.

Förbränningskällor ger ett stort bidrag till luften i stadsmiljöer, både genom direkta utsläpp och åldrade partiklar som transporteras dit. Det finns idag regler för hur höga partikelhalterna får vara i stadsmiljöer och om för höga halter uppmäts

måste åtgärder vidtas. För att öka förståelsen kring partikelsammansättningen i luften och partikelkällor i den urbana miljön, genomfördes fältmätningar i centrala Köpenhamn. Resultaten från fältstudien visar att stadsluften domineras av två partikeltyper med olika fysikaliska egenskaper. Den ena typen var aggregerade partiklar från trafiken, den andra typen var sfäriska partiklar. När det blåste västliga vindar dominerades aerosolen av aggregerade partiklar medan både partikeltyperna förekom i större utsträckning när det blåste från kontinenten. Sotpartiklarnas fysikaliska egenskaper sammanföll med fysikaliska egenskaper hos sotpartiklar från dieselavgaser studerade i laboratoriemiljö.

1 Introduction

1.1 Sources, health impact and climate effects of anthropogenic combustion emissions

Primary and secondary aerosol emissions from anthropogenic combustion sources such as vehicles and biomass combustion contribute significantly to the global aerosol burden (Volkamer et al., 2006; Kocbach-Bølling et al., 2009). The influence from anthropogenic combustion on the ambient aerosol is higher close to the source, which often is in densely populated areas. Biomass combustion aerosol emissions can regionally be a dominating source of ambient particulate matter (PM) during the winter (Krecl et al., 2008). Secondary organic aerosol (SOA) from mobile sources gives an important contribution to the ambient PM in and downwind urban areas (Tkacik et al., 2014).

A large number of epidemiological studies have shown that exposure to particulate emissions from anthropogenic combustion is associated with increased mortality and morbidity due to cardiovascular and pulmonary diseases (Dockery et al., 1993; Brook et al., 2010; Ruckerl et al., 2011). Hoek et al. (2002) concluded that people living close to major roads had a higher risk of mortality and morbidity due to cardiovascular diseases. Particulate emissions from traffic were considered a probable cause of the increased risk. The relative risks from exposure to the soot dominated traffic aerosol, determined in Hoek et al. (2002), were significantly higher than the relative risk from exposure to PM in general. Because of this, it is likely that exposure to soot-dominated aerosol has a larger impact on public health than PM in general, and should therefore merit special consideration, for example in emission mitigation efforts. Salvi et al. (1999) demonstrated that short term exposure to high concentrations of diesel exhaust particles in a chamber caused inflammatory responses in the lungs of the test persons. Occupational diesel exhaust exposure has been linked to increased cancer risk and diesel exhaust has been classified as a carcinogen by the International Agency for Research on Cancer (Benbrahim-Tallaa et al., 2012). Exposure to biomass combustion aerosol in laboratory studies has been shown to induce potential negative health effects such as inflammation, cytotoxicity and arterial stiffness (Barregard et al., 2006; Jalava et al., 2010; Unosson et al., 2013).

The best estimate of the net contribution of aerosol particles on the global radiation budget is negative, i.e. aerosol particles contribute to cooling of the climate (Blanco et al., 2014). However there are still large uncertainties regarding the magnitude of the contribution (Blanco et al., 2014). Particles with a similar diameter as the wavelength of visible light (400-700 nm) are effective in scattering the incoming solar radiation, which has a cooling effect on the climate. The accumulation mode of ambient aerosol often overlaps with the wavelength of visible light and is primarily composed by organic aerosol, nitrate and sulfates. Ambient aerosol also affects climate indirectly through formation of clouds. Black carbon (BC) and brown carbon (BrC) components in addition absorb the incoming solar radiation, which leads to an increase in radiative forcing (Bond et al., 2013; Saleh et al., 2013). Organic aerosol emitted from biomass combustion has "brown" components, the combustion conditions determining the brownness of the emissions are unknown, but Saleh et al. (2014) showed that the brownness, i.e. absorption of lower wave lengths by the organic aerosol (OA), increased with increasing BC to OA ratio. Chung et al. (2012) suggested that organic aerosol when condensed on a soot core might focus incoming radiation towards the soot core to amplify BC absorption, the so called lensing effect. There are clearly some knowledge gaps here, why studies of mixing state and morphology of biomass combustion aerosol particles can be motivated.

Small-scale biomass combustion is a significant heat source for many people in northern and central Europe and the United States and has been promoted as a climate friendly option to fossil fuels. However, increased use of biomass combustion implies increased PM emissions in environments where people reside. Brandt et al. (2011) modelled the contribution of biomass combustion PM to the urban air and found that the concentrations of PM_{10} were higher in areas with dense use of biomass-fuelled heating appliances than in the city center. Fountoukis et al. (2014) predicted that if all of the residential wood combustion in Europe were replaced with new pellet burning techniques, the mass concentrations of elemental carbon (EC) would decrease by 50% in large parts of Europe and the mass concentration of OA would decrease by 60% in urban environments.

Particulate emissions from modern biomass combustion appliances fueled with pellets, where the combustion is fairly controlled, are commonly dominated by alkali salts (Boman et al., 2011). The emissions from older technologies such as wood stoves are to a much larger extent composed of black carbon and organic aerosol (Pettersson et al., 2011). The composition of the aerosol is dependent on operation mode, fuel and the characteristics of the appliance. Polycyclic aromatic hydrocarbons (PAHs) are a subset of the organic aerosol that have merited special interest since some PAH species are or are suspected to be carcinogenic (IARC, 2010). Jalava et al. (2012) studied toxicological responses from cells exposed to PM from different combustion appliances and found that aerosol emitted by appliances with less efficient combustion induced more toxic responses, those

appliances also had the largest emission factors of PAHs. The emissions of PAHs are dependent on the combustion conditions, hot air starved combustion favors PAH emissions (Pettersson et al., 2011; Tapanainen et al., 2012). Previous studies of PAH emissions have been performed using off-line analyzing techniques. To enable a better understanding of the mechanisms of PAH formation, high time resolution studies are needed.

Atmospheric transformation of aerosol changes the chemical and physical characteristics of ambient particles. Organic compounds emitted in the gas-phase from combustion sources become oxidized, which reduces their vapor pressure and allows condensation on existing particles (Donahue et al., 2006). PM formed in the atmosphere from the degradation of organic compounds is referred to as secondary organic aerosol (SOA) (Hallquist et al., 2009). SOA is believed to have a net cooling impact on the global climate, but the uncertainties regarding climate effects, formation mechanisms, sources and emissions factors are still very high (Hallquist et al., 2009).

Recently there has been a debate about which anthropogenic sources that contribute to the ambient SOA production. Gentner et al. (2012) suggested that diesel vehicles were the dominant source of anthropogenic SOA in California, but also stated that both diesel and gasoline powered vehicles were of importance for the ambient SOA production in California. Bahreini et al. (2012) concluded that diesel vehicles in the Los Angeles basin had no impact on the formation of anthropogenic SOA, instead emissions from gasoline vehicles were thought to be a major source. To improve the understanding of traffic related primary and secondary emissions there is a need for laboratory studies on SOA formation from vehicle emissions. Particularly from gasoline exhaust, more knowledge about SOA formation mechanisms and emission factors is needed.

The health impact of aerosol aging is not well known. Only a few studies have been carried out to this day about the effect of aging on the toxicological properties of the aerosol (Gaschen et al., 2010; Kunzi et al., 2013). Kocbach-Bølling et al. (2009) suggested in a review on health effects of biomass combustion aerosol that atmospheric alterations could affect the biological activity of the PM, which could in turn increase or decrease the toxicity of the aerosol. They also stated that the effect of atmospheric aging on biomass combustion aerosol characteristics needed more investigation.

The urban aerosol is a complex mixture of locally emitted and long range transported particles. Traffic and biomass combustion are local sources of particle emissions often containing a substantial fraction of soot agglomerates. The morphology of the soot particles are altered due to atmospheric aging, which affects the optical and hygroscopic properties of the agglomerate (Pagels et al., 2009), which could in turn alter the health and climate impact of soot particles.

Detailed characterization of the urban aerosol is needed to better understand its origin, morphology and mixing state.

1.2 Aims

The overall aim of the research presented in this thesis was to increase the knowledge of the characteristics of particle emissions from anthropogenic combustion with the long term goal to improve the knowledge of their effect on public health and global climate. This was achieved by studying the physical, chemical and toxicological characteristics of the particles and how these are changed due to altered combustion conditions and upon atmospheric aging. The more specific scientific goals were:

- To develop and implement new methods for aging of combustion aerosol at laboratory scale.
- To investigate secondary organic aerosol formation in emissions from gasoline passenger vehicles in order to determine: emission factors, the ratio between secondary and primary emissions and the contribution of traditional light aromatic precursors to the formed secondary aerosol.
- To determine how the combustion conditions of small-scale wood combustion affect the emissions of PAHs and organic aerosol.
- To determine the mass-mobility relationship and morphology for particles emitted from small-scale biomass combustion during different phases and combustion conditions.
- To investigate how ozone initiated aging and combustion conditions affect the characteristics and toxicity of particles emitted from small-scale wood combustion.
- To investigate the mass-mobility relationship and mixing state of urban aerosol particles, to improve the understanding of the characteristics and sources of particles in urban environments.

2 Combustion emissions

Combustion is the process where a fuel (solid, liquid or gaseous) is ideally oxidized to carbon dioxide and water, and the energy stored in the chemical bonds of the fuel is released. However, no ideal combustion situations exist, where all the carbon and hydrogen are completely oxidized, but the combustion can be more or less complete. Important criteria for achieving near-complete combustion are sufficiently high temperature, the right air to fuel ratio and sufficient mixing of air and fuel. Failure to comply with these criteria leads to more incomplete combustion. Potential impurities in the fuel such as alkali metals in solid wood fuel or sulfur in petroleum based fuel, may or may not be oxidized in the combustion process and emitted in the exhaust in different forms, often in the particle phase.

2.1 Emission regulations

Vehicle (light and heavy duty) emissions are regulated by the European emission standards issued by the European Union. The first standard (Euro 1) was implemented in 1992. The European emission standards regulate the emissions of nitrogen oxides (NO_x), total hydrocarbons, non-methane hydrocarbons, carbon monoxide (CO) and particle mass and in a few cases number concentration. The emissions levels are measured during a specified test cycle. The regulation on pollutants has been sharpened in each new version of the emission standard and is applied to new vehicles sold after the implementation date. The emission regulation on PM has in principal required the implementation of particulate traps in diesel passenger vehicles. PM was at first not regulated for gasoline vehicles, but the latest standards (Euro 5 and 6) have the same limit of PM for directly injected gasoline passenger vehicles as for diesel vehicles. For more information go to the EUR-Lex data base (EUR-Lex, 2014).

Emissions from small-scale biomass combustion are currently less strict regulated. However presently there are discussions on European level on how to impose more stringent emissions values from 2018 or later. Germany has taken the lead and put in place new regulation emission limit values (ELVs) for several air pollutants – including PM – for boilers and stoves. As of January 2015, stoves will have to comply with more stringent ELVs, ranging between 20 mg m^{-3} and 40 mg

m^{-3} depending on the type of fuel used. Inspections have been extended to all stoves above 4 kW (previously this was set at 15 kW). This is expected to significantly reduce PM emissions from domestic heating. (EEB, 2014)

2.2 Nitrogen oxides (NO_x)

Nitrogen oxide (NO) is formed during oxygen rich high temperature combustion. NO emissions are an environmental issue causing acidification and it is desirable to reduce them. The chemical reaction forming NO is caused by the high temperature that causes nitrogen and oxygen molecules in the air to react to form NO (Glassman and Yetter, 2008). NO may also originate from nitrogen rich fuels like some types of biomass. Nitrogen oxide plays an important role in atmospheric chemistry, not only does it cause acidification, it is also an important reactant in SOA formation. Nitrogen oxide is also monitored as a tracer for particle emissions from traffic since it is fairly easy to monitor and has shown good correlation with for example soot emissions from diesel cars.

Nitrogen dioxide (NO_2) is formed from the oxidation of NO and can be harmful for public health. Long term exposure to NO_2 has been linked to increased mortality and even though it is often co-emitted with other pollutants, it may still have an independent negative health impact (Faustini et al., 2014).

2.3 Primary organic aerosol

Primary organic aerosol (POA) is commonly defined as the organic aerosol emitted to the ambient air in particulate form, directly from the source. POA is often formed from large organic molecules that are in the gas phase in the combustion zone but are transferred to the particle phase during cooling of the emissions in the exhaust line. In biomass combustion, organic aerosol is primarily emitted during low temperature combustion (for example humid wood), where pyrolysis products are not sufficiently oxidized in the combustion zone. Emissions of POA from batch-wise biomass combustion also occur right after fuel addition (Kocbach-Bølling et al., 2009). Figure 1 shows a transmission electron microscopy (TEM) image of particles from the fuel addition phase. The POA from the fuel addition is emitted as spherical organic particles called “tar balls”. POA from low temperature biomass combustion is often dominated by degradation products of lignin and cellulose (Orasche et al., 2013).

Primary organic aerosol is also emitted from engines, where it mainly originates from hydrocarbons in lubricant oil that escapes oxidation in the cylinder (Sakurai et al., 2003).

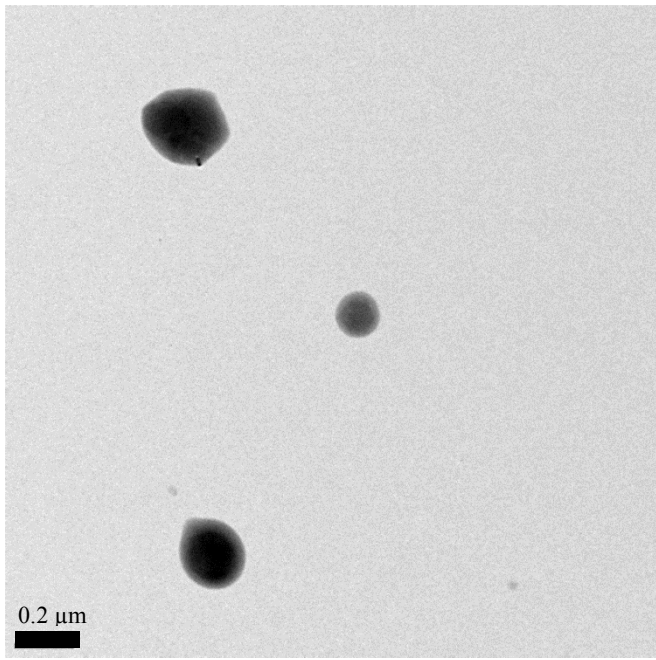

Figure 1
TEM image of particles emitted from fuel addition in a wood stove. They are spherical organic particles, referred to as "tar balls", from the experiments in Paper III.

Polycyclic aromatic hydrocarbons (PAHs)

Polycyclic aromatic hydrocarbons (PAHs) are soot precursors that are often co-emitted with soot, in the gas phase or as coating on the soot particle. Smaller PAHs with two or three rings are most likely found in the gas phase while larger PAHs are often found in the particle phase, due to their lower vapor pressure. The emissions of PAHs from biomass combustion increases at hot air starved conditions during high burn rates (Pettersson et al., 2011; Tapanainen et al., 2012; Orasche et al., 2013).

Brown carbon (BrC)

It was previously believed that organic aerosol did not absorb light, but recent studies have shown UV absorption for organic aerosol from biomass burning. Lack et al. (2012) examined the light absorption of PM in emissions from a wild fire and found that externally mixed organic aerosol contributed to a significant fraction of the absorption of 404 nm (blue) light. Chen and Bond (2010) suggested that brown carbon or light absorbing organic carbon (OC) are rather large, but presently unidentified molecules and that the production of BrC increased with higher combustion temperature. This is indirectly supported by the findings in Saleh et al. (2014), who found that the absorption of OA emitted from biomass combustion increases with increasing BC to OA ratio.

2.4 Soot

Soot particles as found in the ambient air often have an agglomerated structure (Figure 2) built up by primary particles. The primary particles are composed by graphitized carbon, arranged in layered aromatic structures.

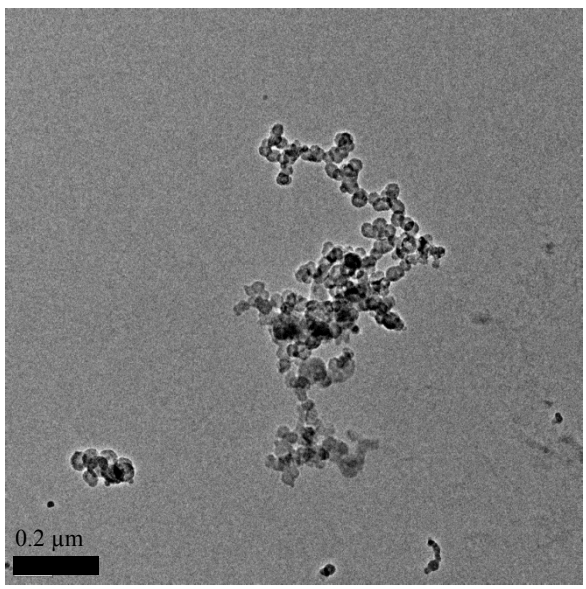

Figure 2
TEM image of a soot agglomerates emitted from a wood stove during the intermediate (flaming) phase from experiments in Paper III.

Soot or black carbon (BC) is formed during the combustion of fuels containing carbon, such as biomass or petrochemical products. Although a lot of progress has been made in the understanding of soot formation, there are still large gaps (Wang, 2011). Soot is formed under hot fuel rich conditions where small hydrocarbons are more likely to collide with other hydrocarbons than to be oxidized (Lighty et al., 2000). The small hydrocarbons collide to form a benzene ring that continues to grow into polycyclic aromatic hydrocarbons, which then grow into larger aromatic molecules. Particles are formed by inception, typically 1-2 nm consisting of about 160 carbon atoms. The particles grow through surface reactions and by colliding with other particles and coalesce upon contact, which keeps the spherical shape intact. When the time in-between collisions becomes faster than the coalescence time, the primary particles will start to form aggregates (Lighty et al., 2000). The size of primary particles in soot aggregates is typically 10 to 30 nm.

Mass mobility relationship and mixing state

The mass of soot particles is not proportional to the cube of the mobility diameter, like spherical particles, due to their agglomerated structure (Virtanen et al., 2002; Park et al., 2003). Equation 1 describes the mass-mobility relationships of agglomerated particles: m_{agg} is the mass of the agglomerate, K is a constant, d_{me} is the mobility equivalent diameter and ε_m is the mass-mobility exponent (Virtanen et al., 2002; Rissler et al., 2013). The effective density (ρ_{eff}^{I}) (Equation 2) is the ratio of the mass (m) of the agglomerate to the volume of a sphere with d_{me} as the diameter. Substituting m_{agg} in Equation 1 with the expression for ρ_{eff}^{I} gives Equation 3, which describes the effective density as a function of mobility diameter, where C is another constant. Figure 3 shows the mass-mobility relationship from a laboratory study on fresh soot from a diesel vehicle and a soot generator (Malik et al., 2011). The black line in Figure 3 is fitted from a mass mobility relationship for the soot emitted from a diesel engine (John Deere, 75 kW) in Park et al. (2003), the fitting parameters are C=16.18 and ε_m=2.32. Rissler et al. (2013) stated that diesel soot agglomerates with <10% volatile coating has a mass mobility exponent of 2.3 ±0.1. For fresh soot with larger organic coatings and upon condensation in the atmosphere, the mass mobility exponent will typically increase towards 3.0 and the effective density will gradually increase towards the material density (Pagels et al., 2009).

$$m_{agg}(d_{me}) = K \cdot d_{me}^{\varepsilon_m} \qquad (1)$$

$$\rho_{eff}^{I} = \frac{m}{\frac{\pi}{6} d_{me}^{3}} \qquad (2)$$

$$\rho_{eff}^{I}(d_{me}) = C \cdot d_{me}^{\varepsilon_m - 3} \qquad (3)$$

The mixing state of an aerosol refers to how chemical components mix between particles at given size. There two extremes: internal mixing (all particles in a size class or mode have the same mixed composition) and external mixing (each particle class or mode is composed of a single species) (Textor et al., 2006). An aerosol with an external mixture with regards to mass-mobility relationship, consists of particles with at least two different effective densities, at a given mobility diameter.

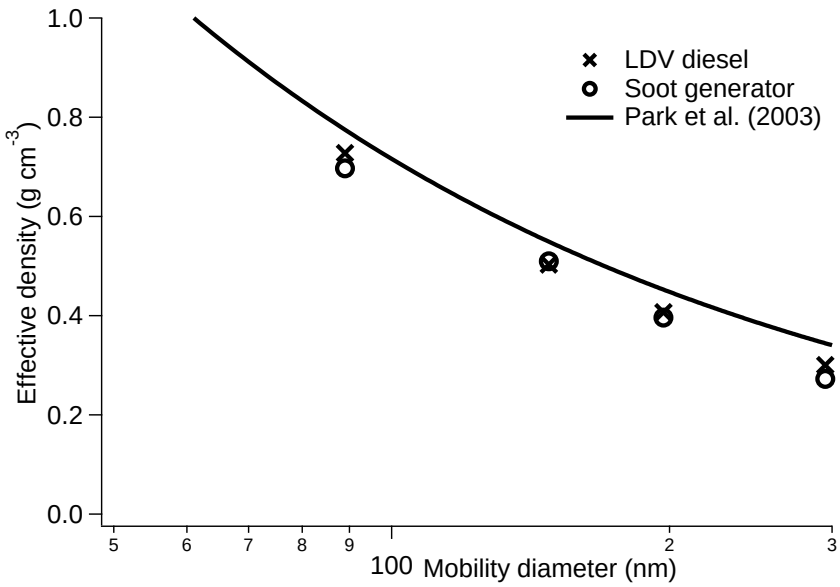

Figure 3
Effective density as a function of mobility diameter for light duty vehicle (LDV) diesel soot and soot particles generated from a soot generator described in Malik et al. (2011). The solid line is fitted from effective density data (John Deere disel engine) from experiments presented in Park et al. (2003).

2.5 Inorganic emissions

Inorganic particles in biomass combustion emissions

In modern biomass combustion appliances like pellets and woodchip boilers, it is generally possible to achieve a more complete combustion than in older techniques like wood stoves. Particulate emissions from complete biomass combustion mostly contain inorganic compounds, since the carbon atoms have been oxidized and mainly emitted as carbon dioxide (Kocbach-Bølling et al., 2009). The alkali metals originate from nutrition species that the biomass absorbs during its growth. Potassium is typically the dominating alkali metal in biomass combustion emissions. Boman et al. (2004) studied the chemical composition of the particulate emissions from three different pellet combustion appliances, using six different fuels and found that the three most frequent alkali salts were KCl, $K_3Na(SO_4)_2$ and K_2SO_4. Boman et al. (2004) also found zinc oxide in the particle phase. Recent studies found that zinc oxide formed the inner nuclei of the ash particles and that alkali salts condenses on the nuclei (Yang et al., 2013; Torvela et al., 2014). During optimal combustion, when the emissions of carbonaceous PM is low, inorganic ash particles are found in the ultra-fine mode (<100 nm), but during less optimal conditions, inorganic ash particles can be internally mixed with soot and organic aerosol in the accumulation mode (> 100 nm) (Torvela et al., 2014).

Inorganic particles in engine emissions

The fuel or lubricant oil may contain metals such as Al, Ti and Cu, which are emitted as metallic ash transferred to soot particles by coagulation and/or condensation or are nucleated to form independent particles (Kittelson, 1998; Maricq, 2007). Engine emissions may also contain sulfuric acids and sulfates due to sulfur content in the fuel, though most of the sulfur is emitted as SO_2 (Kittelson, 1998). In the European Union there is a limit to the sulfur content in the fuel, which has significantly reduced the sulfur containing emissions from vehicles.

2.6 Secondary organic aerosol (SOA) formation

Secondary organic aerosol (SOA) is formed from atmospheric reactions initiated by UV-light or tropospheric ozone, and degrade gas-phase biogenic or anthropogenic organic compounds (for example volatile organic compounds; VOCs) into low volatility oxidized compounds. The magnitude of atmospheric SOA concentration is of major importance for determining the aerosol effect on

the global radiation balance (Monks et al., 2009). There are still major uncertainties when it comes to estimating the SOA production rates from both biogenic and anthropogenic sources (Hallquist et al., 2009).

The degradation of organic compounds and SOA formation is a very complex process that involves thousands of reactions and several radicals (Hallquist et al., 2009). Below is a short summary of some of the most important mechanisms. Photolysis induced by UV-light leads to the formation of hydroxyl radicals (OH). The OH radicals degrade the VOCs to oxidized reactions products, in the first major step peroxy-radicals. The VOC to NO ratio affects the SOA yield for a given precursor (Hildebrandt et al., 2009). At high VOC to NO ratios the peroxy-radicals react with HO_2 resulting in relatively high yields for SOA formation. If NO is typically higher than a few ppb the degradation of the VOCs takes an alternate pathway, where the formed peroxy-radicals reacts with NO and nitrated reaction products are formed (Hallquist et al., 2009). The nitrated reaction products typically have higher vapor pressures resulting in low SOA yield. Ozone-initiated chemistry is similar to photo-oxidation chemistry in the sense that it leads to formation of hydroxyl- and peroxy-radicals (Hallquist et al., 2009).

The SOA formation from traditional SOA precursors (for example light aromatics from combustion sources) is dependent on the level of OH radicals present (Song et al., 2007). In laboratory studies the cumulative OH exposure can be used to normalize the SOA formation, which enables comparisons between different smog chambers or potential aerosol mass chambers (PAM). A cumulative OH exposure of 10^6 cm^{-3} h is equivalent to about one hour of atmospheric exposure on a winter day in Northern Europe.

Donahue et al. (2006) introduced a framework called the volatility basis set (VBS), a tool for describing gas-particle phase interaction of organic compounds. The VBS classifies the organic components into volatility bins depending on the magnitude of their saturated vapor concentration (which is derived from the saturation vapor pressure). For example at a given concentration of OA it is possible to estimate what fraction of an organic component that would partition to the particle phase. Additionally one can estimate the phase distribution and SOA yield as the saturation vapor pressure decreases due to atmospheric processing of organic compounds.

3 Materials and Methods

The results presented in this thesis are focused on experiments with in-use light duty vehicles, conventional biomass combustion appliances and measurements in an urban environment. Table 1 shows a summary of the sources and methods used in Paper I-V.

Table 1
A summary of the aerosol sources and main experimental methodologies used in the thesis.

Paper	Research focus	Aerosol source	Sampling mode and aging	Main characterization instruments
I	SOA formation from gasoline vehicle exhaust	Idling gasoline vehicles, light aromatic precursors	Photo-oxidation in smog chamber	Scanning mobility particle sizer (SMPS), AMS, PTR-MS
II	Transient PAH emissions from wood stoves	Conventional wood stove	Transient measurements in diluted flue gases	AMS
III	Mass-mobility relationship and mixing state of biomass combustion aerosol	Conventional wood stove, pellet combustion appliances	Measurement of isolated combustion phases in steel chamber, no aging	DMA-APM
IV	Chemical and toxicological properties of fresh and aged biomass combustion aerosol[a]	Conventional wood stove	Dark aging in steel chamber with O_3	DGI
V	Mass-mobility relationship and mixing status of urban aerosol	Urban street-level aerosol	Outdoor measurements in wintertime	DMA-APM

[a] The toxicological tests were performed by Kuopio Univesity.

3.1 Smog chambers

Flexible Teflon bags, referred to as smog chambers or simulation chambers have been used over the last few decades to simulate atmospheric reactions in a controlled environment. The advantage of using Teflon is the high UV transmission (>90%) (Paulsen et al., 2005), which enables the light sources to be placed outside the chamber, which prevents contamination of the aerosol. The flexibility of the chamber also makes it possible to maintain a stable pressure in the Teflon chamber when the volume is decreased upon aerosol sampling.

The smog chamber in the aerosol laboratory at Lund University was used in the gasoline SOA experiments presented in Paper I, in controlled processing of diesel exhaust reported in this thesis and hygroscopicity of aged diesel soot (Wittbom et al., 2014). Modeling of the chemistry and aerosol dynamics in the chamber is presented in Roldin et al. (2014).

Implementing the smog chamber system, we specified the performance of a number of parameters to make sure that the overall performance was up to par with similar systems in other laboratories. Important parameters for successful aging experiments are temperature stability over the whole experiment, photolysis rate and low background concentration of particles and gases.

The characteristics of the Lund smog chamber are listed in Table 2 along with the characteristics of two established chambers from the literature. The temperature in the Lund smog chamber increased about 2 °C during a five hour experiment, due to the heat released from the UV light source. The photolysis rate (J_{NO_2}) of 0.2 min $^{-1}$ induced by the UV irradiation was sufficient to achieve a cumulative OH exposure equivalent to several hours of atmospheric aging. The light spectrum of the UV source ranged between 320 and 380 nm, peaking at 350 nm. The background concentration of particles were in most experiments <<100 cm^{-3} and were negligible in comparison to the initial concentration of sulfate seeds (20 000-25 000 cm^{-3}). The smog chamber was also tested in several blank experiments where purified air was taken through the heated sampling line, where exhaust was normally diluted and injected from the vehicles. This was done to make sure the formation of SOA from background concentration of VOCs was negligible. The SOA mass concentration in the chamber in a blank experiment was <0.1 µg m^{-3} after several hours of radiation.

Due to electrostatic forces and other deposition mechanisms, aerosol particles deposit on the wall of smog chambers (McMurry and Rader, 1985). The wall losses are more pronounced in smaller smog chambers, like the one at Lund University, due to lower volume to surface ratio. Wall losses had to be accounted

for in order to make a useful estimate of the SOA formed. The wall loss correction method used is further described in Paper I and in Hildebrandt et al. (2009).

Table 2
Characteristics of the Lund University smog chamber, compared to two similar smog chamber setups, the PSI chamber is presented in (Paulsen et al., 2005) and the California Institute of Technology chamber is presented in Cocker et al. (2001).

	Dimensions W*L*H (m)	**Temperature (°C)**	J_{NO_2} **(min^{-1})**	**Background concentration (# cm^{-3})**
Lund University	2.1*1.5*1.8	(20-25) ± 2	0.2	<100
PSI	4*5*4	(15-30) ± 1	0.12	<20
Cal Tech	2.5*3*3.7	(18-50) ± 1	N/A	N/A

Generation of vehicular emissions to the smog chamber

Initial tests were performed on ten gasoline-powered light duty vehicles and three diesel-powered light duty vehicles, using a flame ionization detector (FID) to measure VOCs and a portable flue gas analyzer (Testo, model 350 XL) for NO_x and CO measurements. Out of them three gasoline cars were selected, one Euro 2, one Euro 3 and one Euro 4 and one diesel car (Euro 2). The vehicles' exhaust was sampled into the smog chamber using a Dekati ejector dilutor. The injection times for the gasoline vehicles were typically 5-10 minutes and 90 seconds for the diesel vehicle. The ambient temperature was typically a few degrees below zero centigrade. A schematic of the smog chamber setup is illustrated in Figure 4.

In the experiments presented in Paper I, emissions from three different idling gasoline vehicles were sampled into the smog chamber for the aging experiments. The standard operation mode was referred to as "cold idling" where the car was started with a cold engine, driven for 3 minutes on a standardized circuit before being put on idle. A "cold start" experiment was also performed where the emissions were sampled into the smog chamber from first ignition. The cold idling mode was developed to represent a realistic emission scenario in winter time in an urban environment and showed good repeatability in-between experiments.

Photo-oxidation experiments on the emissions form the diesel car and light aromatic precursors are described in detail in Wittbom et al. (2014). Here, additional results on the effects of atmospheric processing on the mass-mobility relationship of diesel soot will be reported.

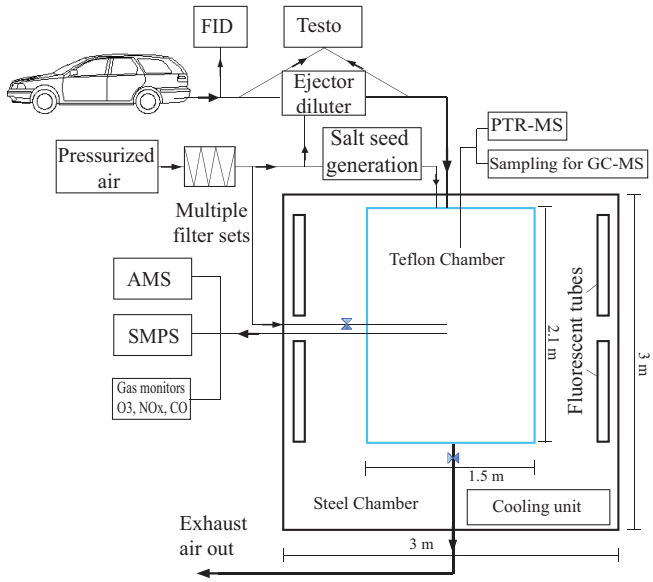

Figure 4
A schematic figure of the setup used for aging of gasoline exhaust in Paper I.

3.2 Small-scale biomass combustion appliances and operation modes

There are several types of biomass combustion appliances for domestic heating. The heat can be transferred directly to the room from the stove or the chimney, or through a heat exchanger to an accumulator tank connected to a warm water system in the building. Common fuels are wood logs, pellets and wood chips. In this thesis, the results from emission measurements from one wood stove, one pellet stove and one pellet boiler are presented.

A conventional wood stove sold on the Swedish market was used as the main source of PM emissions in Paper II, III and IV. The stove is further described in Pettersson et al. (2011). The fuel used was birch wood logs. Table 3 presents a summary of how the combustion conditions in Papers II, II and IV were achieved.

Table 3
Summary of the combustion conditions for the wood stove used in Papers II, II and IV. Note that different abbreviations are used for the nominal combustion mode in the different papers. Oxygen minimum denotes the lowest oxygen concentration measured during the cycle.

Operation mode (abbreviation used)	Phases included	Wood mass /number of logs	Oxygen minimun (%)
		Paper II	
Nominal burn rate (NB)	Full cycle (add fuel+ intermediate + burn out)	~1.8 kg/2 logs (15% moisture)	7
High burn rate (HB)	Full cycle	~2-2.5 kg/6-7 logs (15% moisture)	2
		Paper III	
Nominal burn rate (NB)[a]	Full cycle	~2.5 kg/ 3 logs (15% moisture)	8
High burn rate (min) (HB-min)	Full cycle	~3.0 kg/ 7 logs (7% moisture)	4
High burn rate (max) (HB-max)	Full cycle	~3.5 kg/ 9 logs (7% moisture)	0
		Paper IV	
Nominal burn rate (NOM)	Full cycle	~2.5 kg/ 3 logs (15% moisture)	5
Hot air starved (HAS)	Add fuel + first part of intermediate repeated (High burn rate)	1-3 smaller logs added every 5 minutes	2

[a]Separate phases (add fuel and intermediate) of a nominal combsution cycle were also studied.

Nominal burn rate was achieved by operating the wood stove in accordance with the instructions from the manufacturer. Smaller pieces of wood were used to achieve higher burn rates. By cutting the logs into smaller pieces a higher surface to mass ratio was achieved, which allowed for a faster evaporation of combustible products from the logs. The burn rates were estimated based on the analysis described in Paper II. As an example NB and HB in Paper 2 correspond to burn rates of 1.9 and 2.9 kg h^{-1}. The wood used for the two higher burn rates in the Paper III study had been stored indoors and thus had a lower moisture content, which resulted in faster combustion since less energy was being used to dry the wood in the combustion bed. In the Paper IV experiments the hot air starved (HAS) conditions were achieved by adding smaller wood logs to the combustion bed during the intermediate phase. This operation mode combines the elevated organic emissions during the add fuel phase with a soot and PAH-rich aerosol that is emitted during the first part of the intermediate phase during high burn rate

combustion. An aerosol similar to the HAS case was used in a human exposure study presented in Unosson et al. (2013).

Emissions from pellet combustion appliances were studied in Papers II and III. Two appliances were used, a modern pellet boiler operated at nominal conditions and a pellet stove operated at nominal and hot air starved conditions. Nominal conditions denoted the recommended operation by the manufacturer, while the hot air starved conditions were achieved by lowering the secondary air supply.

The concentrations of O_2, CO and NO in the undiluted flue gases were monitored by a flue gas analyzer (Testo, model 350). In Paper II the AMS sampled directly in the diluted flue gases, the dilution system in the study consisted of a porous tube dilutor and two Dekati ejector dilutors (total dilution 1 500-3 000). In Paper III the flue gases from the wood stove were diluted (~200 times) and transferred to a mixing chamber by means of two Dekati ejector dilutors.

3.3 Methods for generation of fresh and aged aerosol for toxicological studies

The toxicological analysis in Paper IV required at least 10 mg of particle mass $PM_{1.0}$) collected on substrates by a Dekati gravimetric impactor (DGI) (Ruusunen et al., 2011). It was desirable that the fresh and aged aerosol samples could originate from the same experimental batch to avoid uncertainties due to unavoidable small differences in combustion conditions between batches. To achieve this, emissions from the wood stove were diluted and sampled to a 15 m^3 stainless steel mixing chamber. First the fresh aerosol was collected, then ozone was added and a short time for mixing was allowed. Then collection of the aged aerosol stared. Fresh and aged aerosol was collected from wood stove emissions from two different operation conditions, nominal (NOM) and hot air starved (HAS).

The aerosol in the chamber was characterized by several on-line and off-line techniques, including thermo-optical analysis of organic and elemental carbon, tapered element oscillating microbalance and gas chromatography-mass spectrometry (GC-MS) analysis for gas and particle phase PAHs. The aerosol was extracted from the DGI filters and a fraction of it was used for analysis of particle phase PAHs and trace metals. The laser vaporizer aerosol mass spectrometer (SP-AMS) was not available during the initial aging experiments. Instead a replicate experiment was carried out where the ratio of organic aerosol to refractory black carbon (rBC) and the ratio of PAHs to rBC were determined for aging of HAS-mode aerosol.

Toxicological tests

The toxicological tests used in Paper IV were designed and performed by researchers at the Department of Environmental Health at the Finnish National Institute for Health and Welfare in Kuopio, Finland. The process is more extensively described in Jalava et al. (2005), Jalava et al. (2010) and Tapanainen et al. (2012). The biological model was Mouse RAW264.7 macrophages. The cells were exposed to four doses of combustion aerosol (15, 50, 150 and 300 μg ml^{-1}), from fresh and aged nominal combustion aerosol and fresh and aged hot air starved combustion aerosol. The cells were tested for the following toxicological endpoints: cell cycle analysis, cell viability, production of inflammatory mediators and DNA damage (genotoxicity).

3.4 Urban and rural campaigns

The mass-mobility measurements of urban aerosol took place in central Copenhagen at street level. The instrumentation was placed indoors in a street-side building. A mixing volume (residence time one minute) was added upstream the DMA-APM to remove the effect of single vehicles on the sampled aerosol.

The rural campaign was performed at a rural background station 45 km northeast of Copenhagen. The instrumentation was placed inside a heated measurement wagon.

4 Instrumentation

4.1 Technique for measurements of the mass-mobility relationship

The mass-mobility relationship of aerosol particles can be determined using the differential mobility analyzer-aerosol particle mass analyzer (DMA-APM) technique. The DMA selects particles of a given mobility diameter and the APM measures the mass of these particles. To determine the volatile mass of the aerosol, a thermodenuder (TD) was placed between the DMA and APM. The volatile mass was defined as the difference between the masses measured with and without TD for the same initial mobility size. The DMA-TD-APM technique was the main instrumentation used in a laboratory study to characterize biomass burning aerosol in Paper III and in a field study at an urban street-level and rural background location in Paper V.

The DMA-APM technique was first described by (McMurry et al., 2002). The APM consists of two concentrical cylinders that rotate at the same angular velocity in the same angular direction. A voltage (V_{APM}) is applied over the cylinders which creates an electrical field. Since the gap between the cylinders is much smaller than the radius of the outer cylinder, the electrical field can be considered uniform over the gap. Particles with a given mass (the centrifugal force on the particle is equal to the electrical force) are able to exit the APM. Particles that exit the APM are detected by a condensation particle counter (CPC) and a voltage distribution is formed. A schematic of the DMA-APM setup is given in Figure 5.

$$m = \frac{qV_{mean}}{r^2\omega^2 \ln(\frac{r_2}{r_1})} \qquad (4)$$

The DMA-APM was operated by stepping the voltage (V_{APM}) using a custom made *Labview*™ program, developed by the University of Minnesota, Texas A&M University and Lund University. The program allows continuous operation of the instrument. The DMA-APM data were evaluated using a custom made *MATLAB* program. The transfer function of the DMA defines the probability of a particle as a function of mobility to exit the instrument at a given setting. The DMA transfer function is triangular shaped. The transfer function for the APM resembles the shape of a triangle with the top angle cut off. Convoluting the two

transfer functions results in the transfer function for the DMA-APM system. It can be approximated with a normal distribution (Emery, 2005). The program attempts to fit a normal distribution function to the measured voltage distribution acquired from the APM. The *MATLAB* program is also capable of fitting two normal functions to one spectrum if there is a bimodal mass distribution (externally mixed aerosol). The fitted mean value (V_{mean}) of the voltage distribution is used for calculations of mass (m) according to Equation 4, where r_1 is the radius of the inner cylinder and r_2 is the radius of the outer cylinder, $r = (r_1+r_2)/2$, q is the particle charge and ω is the angular velocity of the rotating cylinders.

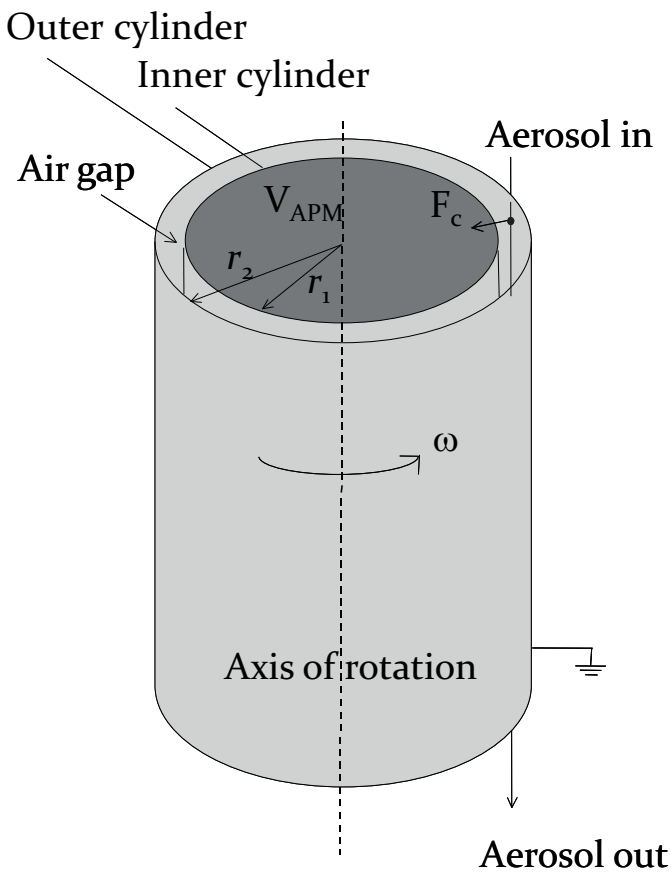

Figure 5
Schematic and operation principle of the APM, F_C denotes the centrifugal force.

Calibration of the DMA-APM

The DMA-APM is calibrated using monodisperse polystyrene latex (PSL) spherules (Duke Scientific Corp.). The results from the calibration are applied to the fitted APM voltage from a measurement (V_{mean}) according to Equation 5, where the theoretical density of PSL particles (ρ_{PSL}) is 1.054 g cm^{-3} and V_{PSL} is the APM voltage derived from the calibration (McMurry et al., 2002). This results in a true effective density (ρ_{true}) of the measured particles.

$$\rho_{true} = \rho_{PSL} \frac{V_{mean}}{V_{PSL}} \quad (5)$$

Table 4
Calibration data from two separate campaigns of DMA-APM measurements at two different locations, nine months apart. The effective measured density of the PSL spheres (ρ_{cal}) is derived from V_{PSL}.

Mobility diameter PSL (nm)	DMA voltage (nm)	V_{PSL} (V)	ρ_{cal} (g cm^{-3})
	Biomass combustion campaign (Paper III)		
102	1045	103.3	1.097
102	1045	102.9	1.093
102	1045	102.4	1.087
240	4024	486.7	1.096
240	4024	486.3	1.095
240	4024	486.6	1.096
350	6774	661.2	1.076
350	6774	656.6	1.068
350	6774	659.3	1.073
	Rural campaign (Paper V)		
102	1057	80.3	1.001
102	1057	80.3	1.000
102	1057	80.3	1.000
240	4093	466.2	0.973
240	4093	467.1	0.975
240	4093	466.2	0.973
350	7014	653.6	0.978
350	7014	649.2	0.979

The measured voltage of PSL spherules (V_{PSL}) in adjacent runs at the same mobility diameter, differed only a few percent at most between the runs (Table 4), indicating that the DMA-APM technique has very high precision. The measured effective density of PSL particles differed up to 10% in between campaigns (Table 4). The greatest source of error is probably the sheath flow control of the DMA, an error of 3% in the mobility diameter measurement would cause an error of ~10% in the mass measurement ($m \propto d_{me}^3$).

McMurry et al. (2002) showed that the accuracy of density measurements with the DMA-APM can be done with an uncertainty of less than 5% if the procedure above is followed. We expect to be within that range after applying the PSL correction.

4.2 Aerosol mass spectrometry

A high resolution time of flight aerosol mass spectrometer (HR-ToF-AMS, Aerodyne Research Inc.) (DeCarlo et al., 2006), was used in all of the studies included in this thesis to different extent. In Papers I, III, IV and V the HR-ToF-AMS was equipped with a laser vaporizer (SP-AMS) (Onasch et al., 2012), which allowed detection of refractory material like black carbon. The operation principle is more extensively described in the aforementioned references and just briefly below. The AMS samples particles by means of a vacuum system maintained by five turbo pumps. The sampling flow rate is relatively low ~0.1 lpm. To shorten the residence time in the sampling line in order to avoid particle losses, an auxiliary flow of typically 1.0 lpm was used in the campaigns. Entering the AMS the particle stream is focused by an aerodynamic lens. The constituents of the lens enable high transmission for particles with a vacuum aerodynamic diameter (d_{va}) between 50-500 nm. After the lens, the focused particle beam is chopped up (optional) to measure the time of flight of the particle, from which its vacuum aerodynamic size is determined. The particles are then vaporized by either a 1064 nm laser (SP-AMS) or by a heated (600 °C) Tungsten plate. The vaporized molecules are bombarded by 70 eV electrons from a filament and a fraction becomes ionized. The electrons cause hard ionization, which breaks down the molecules into smaller fragments that travels through the time of flight mass spectrometer which determines the mass (atomic units) to charge ratio (m/z) of the fragments. The intensities at different m/z's form a mass spectrum (MS). Molecules much larger than the fragments can in some cases be determined due to the specific pattern of the MS.

The acquired data was analyzed with *Igor Pro* software and various versions of the plug-in software *Squirrel* and *PIKA*. Standard fragmentation patterns and calibration fractions were used as described in Aiken et al. (2008). For the PAH

quantification in Papers II and IV an algorithm based on careful calibration with PAH standards by Dzepina et al. (2007) was used. The algorithm was based on the way PAHs are fragmented in the ionization process in the AMS, giving them a unique mass spectrum.

Even though improvements have been made there are still some uncertainties regarding the quantification of refractory black carbon in the SP-AMS, hence comparison with other independent techniques is important.

5 Results and discussion

This section highlights the results from the papers included in the thesis and an effort is made to relate the results to other recent publications dealing with the same subject.

5.1 SOA formation from light duty vehicles – Paper I

The contribution of SOA formed from gasoline vehicle emissions to the overall traffic generated aerosol have been considered negligible compared to the primary and secondary emissions from diesel vehicles (Gentner et al., 2012). On the contrary a recent study by Bahreini et al. (2012) concluded that gasoline SOA dominated over diesel SOA in the Los Angeles basin in California. Thus it is clear that more studies were needed about the SOA formation from gasoline vehicle exhaust. Paper I presents to our knowledge the first laboratory study that attempted to quantify the SOA production and its composition from in-use gasoline vehicles.

Apparent mass yield and chemical composition of gasoline exhaust SOA

Light aromatic (LA) VOCs (C_6-C_9) have been pointed out as the main SOA precursors in gasoline exhaust based on smog chamber measurements with unburned gasoline fuel (Odum et al., 1997). Unburned gasoline fuel can contain up to 30% light aromatics. The main SOA precursors in diesel vehicle emissions are recognized to be intermediate volatile organic compounds (IVOCs) and semi-volatile organic compounds (SVOCs) (Robinson et al., 2007; Weitkamp et al., 2007). A total of six (five cold idling and one cold start) aging experiments were carried out in the smog chamber to study the SOA formation from gasoline vehicle exhaust To further elaborate the hypothesis by Odum et al. (1997), we performed two additional experiments where only light aromatic VOCs were injected to the smog chamber.

The relative molar fractions of light aromatics in the exhaust from the gasoline vehicles and in the fuel are shown in Figure 6. The composition of the cold start

experiment is similar to the fuel sample, while the cold idling experiments contain a higher fraction of benzene.

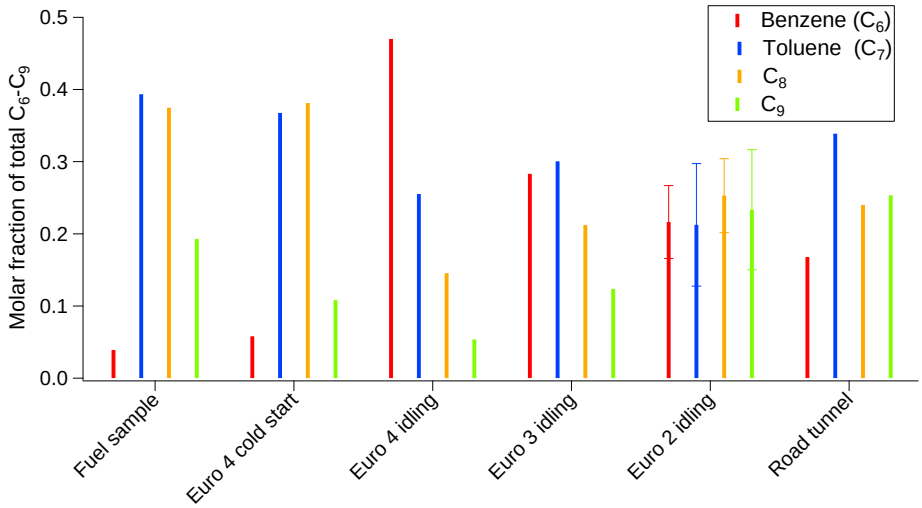

Figure 6
The relative molar fractions of light aromatics of different size measured with GC-MS from the smog chamber experiments before photo-oxidation and a fuel sample. The road tunnel measurement is from a publication by Legreid et al. (2007)

The concentrations of light aromatic VOCs were also monitored on-line throughout the experiments. At the end of the experiment we calculated the apparent mass yield, which is the ratio between the formed SOA mass and the light aromatics mass consumed. Parameterizations (Figure 7) showed that the apparent mass yield in the model experiments with pure light aromatic precursors corresponded to about 60% of the apparent mass yield in the cold idling experiments. This implies that a substantial fraction of the SOA has been formed from additional precursors. The apparent mass yield for the cold start experiment instead followed the parameterization of m-Xylene from Song et al. (2005). Proton transfer reaction-mass spectrometry (PTR-MS) measurements showed that heavier VOCs such as naphthalene were to a larger extent present in the cold idling experiments compared to cold start. Based on the PTR-MS measurements and OH reactivities we concluded that heavier aromatics such as C_{10}, C_{11} aromatics as well as naphthalene and methyl-naphthalenes were important contributors to the additional precursors.

In addition to the results from the apparent mass yield, the SOA AMS mass spectra are also markedly different for the cold idling (higher fraction at m/z=44)

compared to the pure precursor and cold start experiments, as discussed further in Paper I. During a cold start the oxidation catalyst has yet to reach its operation temperature, hence the emissions will contain more unburned fuel (Weilenmann et al., 2009), including light aromatic SOA precursors.

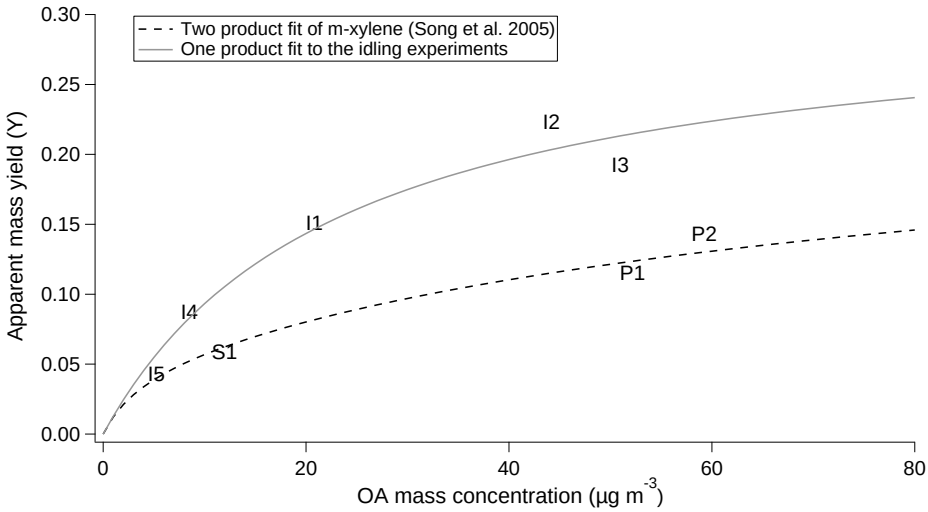

Figure 7
The apparent mass yield from the gasoline experiments in Paper I, plotted against the mass concentration of organic aerosol. The bottom black line is a two product fit to the m-xylene yield from Song et al. (2005). I1-I5 represent cold idling, S1 cold start and P1-P2 the precursor experiments.

SOA formation and POA emissions in gasoline vs diesel exhaust

The differences in combustion technique and chemical composition of the fuel between gasoline and diesel vehicles have implications not only for soot formation and emissions but also for the emission of POA and the production of SOA. Chirico et al. (2010) studied the primary emissions and SOA formation from light duty diesel vehicles and reported emission factors for experiments without particulate filter. The SOA to POA ratio was ~0.14. For the gasoline experiments reported here in Paper I, the SOA to POA ratio was 7-500.

Compared to diesel vehicles secondary organic emissions appears to be of higher importance for gasoline vehicles, which is in agreement with other more recent data in the literature. May et al. (2014) investigated primary emissions (particulate and gaseous) from 64 in-use diesel and gasoline vehicles and found that the ratio

of SOA precursors to primary particulate emissions was an order of magnitude larger for the gasoline vehicles compared to the diesel vehicles examined. Paper I reported that about 10-15% of the hydrocarbons emitted in idling gasoline exhaust were traditional SOA precursors; the corresponding number in diesel exhaust was only about 5% (Schauer et al., 1999).

The primary emission component is today fairly easy to remove with a particle trap and there is also a clear regulation on primary PM through the European emissions standards directive. Even though the oxidation catalyst may remove most gas-phase hydrocarbons (including SOA precursors), the function is limited during cold starts and the time-interval shortly thereafter.

5.2 PAH emissions from small-scale biomass combustion – Paper II

Previous studies of PAHs in aerosol emissions from wood stoves have used filter based collection techniques followed by gas chromatography-mass spectrometry (GC-MS) or similar off-line techniques (Pettersson et al., 2011; Orasche et al., 2012). The advantage of GC-MS is the low detection limit and the ability to distinguish between isomers. A drawback with the use of GC-MS for the analysis of biomass combustion emissions is the lack of time resolved data, which would be of essence to improve the understanding of the mechanisms behind PAH emissions. The idea of using aerosol mass spectrometry to detected and quantify particulate phase PAHs was first presented by Dzepina et al. (2007), who developed an algorithm to distinguish PAHs signals within the mass spectrum. Paper II presents high time resolution AMS-measurements of emissions from full combustion cycles in the conventional wood stove, together with on-line monitoring of oxygen and carbon monoxide in the flue gases.

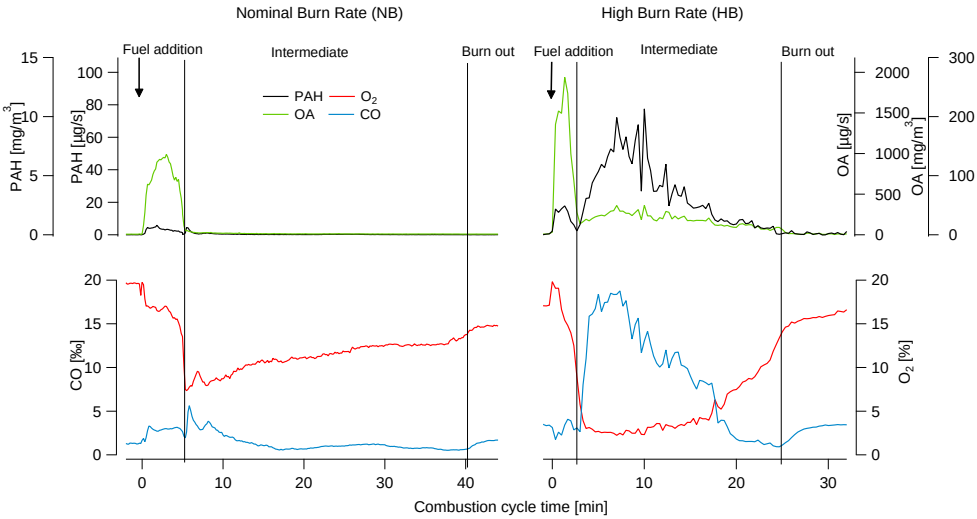

Figure 8
Time series from a nominal burn rate combsution cycle (left) and a high burn rate combustion cycle (right). The upper panel shows the the emissions of PAHs and organic aerosol (OA). The bottom panel shows the flue gas content measured in the smoke stack. The combustion cycle is divided into three phases: fuel addition, intermediate and burn out.

The particulate phase PAHs and the total emissions of organic aerosol (incl. PAHs) is plotted (upper panel Figure 8) during the course of a combustion cycle from fuel addition to the burn out phase for two combustion modes; nominal and high burn rate. Note that there are different scales on the y-axes. During fuel addition there is an emission burst of organic aerosol for both combustion modes. During the intermediate phase there are relatively low emissions of PAHs and organic emissions in the nominal combustion case, while in the high burn rate case the emissions of PAHs increase heavily. Looking at the simultaneous measurements of O_2 and CO in flue gases (lower panel Figure 8), the O_2 concentration in the flue gas drops below 5% and the CO emissions are elevated during that phase. The emissions of organic aerosol and PAHs decrease as the batch of wood logs burn out.

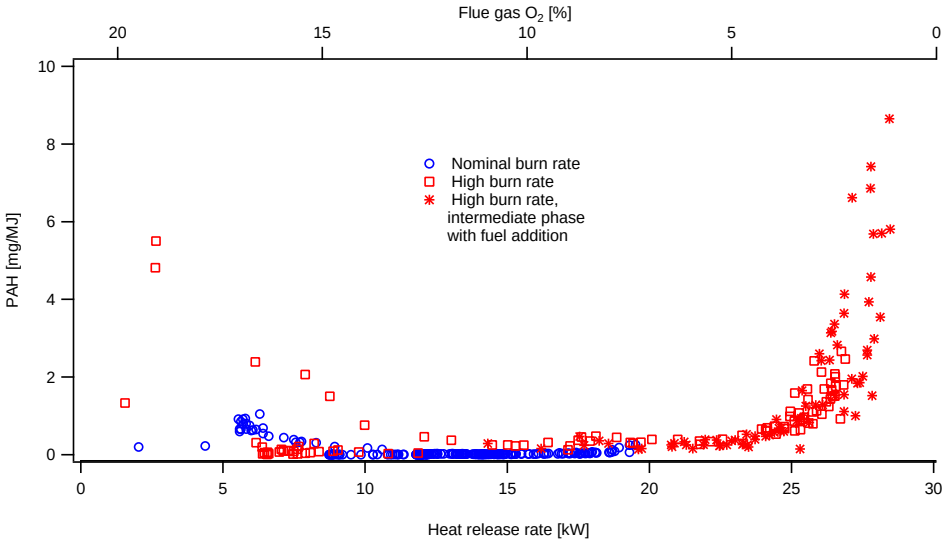

Figure 9
Emissions of particulate PAHs as a function of heat release (lower x-axis) and oxygen concentration in the flue gas (upper x-axis).

Emission factors of particulate PAHs were plotted as a function of instantaneous heat release rate and flue gas oxygen content in Figure 9. The highest emission factors of particulate PAHs correlates (with a few exceptions) with the highest heat release rate in the combustion zone and low (<5%) oxygen concentration. The highest emissions factors were recorded during an experiment where a few small wood logs were added to the intermediate (flaming) phase of a combustion cycle.

The elevated emissions of organic aerosol during the fuel addition phase come from pyrolysis products from the fuel as the wood logs are being heated. As the flaming combustion starts in the wood stove, these emissions decrease because the pyrolysis products are being combusted. The majority of the PAH emissions occurs during the intermediate phase. The increased PAH emissions during this phase in the high burn rate experiment occur simultaneously as low oxygen abundance and correlate to a certain degree with increased CO emissions. The hot air starved conditions during the intermediate phase in a high burn rate experiment clearly favor PAH emissions, which also have been seen by others (Elsasser et al., 2013).

Avoiding combustion conditions with excessive heat release rate and low oxygen abundance would be the most efficient way to reduce the potentially harmful PAH emissions. On-line monitoring of oxygen is much less complicated than monitoring of PAHs. However, the critical point in O_2 concentration when PAH emissions become elevated most likely varies between different combustion appliances.

5.3 Mass mobility relationship and mixing status of biomass combustion aerosol – Paper III

Mass mobility measurements were conducted using the DMA-TD-APM technique on pellet combustion appliances and different operations modes of the conventional wood stove (Table 3). The transient nature of wood stove emissions does not favor measurement techniques with limited time resolution such as DMA-APM, so the wood stove emissions were diluted and transferred to a 15 m^3 steel mixing chamber. The wood stove experiments focused both on single phases of the combustion cycle, where emissions from a single phase were transferred to the chamber and on measurements of the whole combustion cycles. The phases selected were: "fuel addition phase" and "intermediate phase" (Figure 8). For the whole cycle experiments, three operation modes were selected; nominal, high burn rate-min and high burn rate-max. The operation modes are further described in Table 3. The less transient nature of pellet combustion allowed for measurements directly on the diluted emissions.

Mass mobility relationships of the three main particles types found in biomass combustion emissions

The mass-mobility relationships (effective density as a function mobility diameter) from the experiments on the fuel addition phase and the intermediate phase of a wood stove and the continuous operation of a pellet boiler are presented in Figure 10.The three major types of biomass combustion aerosol particle types are illustrated: organic aerosol dominated, soot agglomerates and inorganic ash dominated. The aerosol particles emitted from the nominal operation of pellet appliances had an effective density of ~1.9 g cm^{-3} for all the sizes, which is typical for inorganic ash (salt) particles. The size distribution is shifted towards smaller particles. The particles from the add fuel phase have an effective density of 1.2-1.3 g cm^{-3}, which does not appear to be dependent on mobility diameter. The size distribution is clearly shifted towards larger particles. The mass-mobility relationship from the intermediate (flaming) phase aerosol shows a decreasing effective density with increasing mobility diameter, which is to be expected since the flaming phase usually is dominated by soot particles. The solid line in Figure 10 is the mass-mobility relationship from a measurement on soot from a diesel engine (Park et al., 2003).

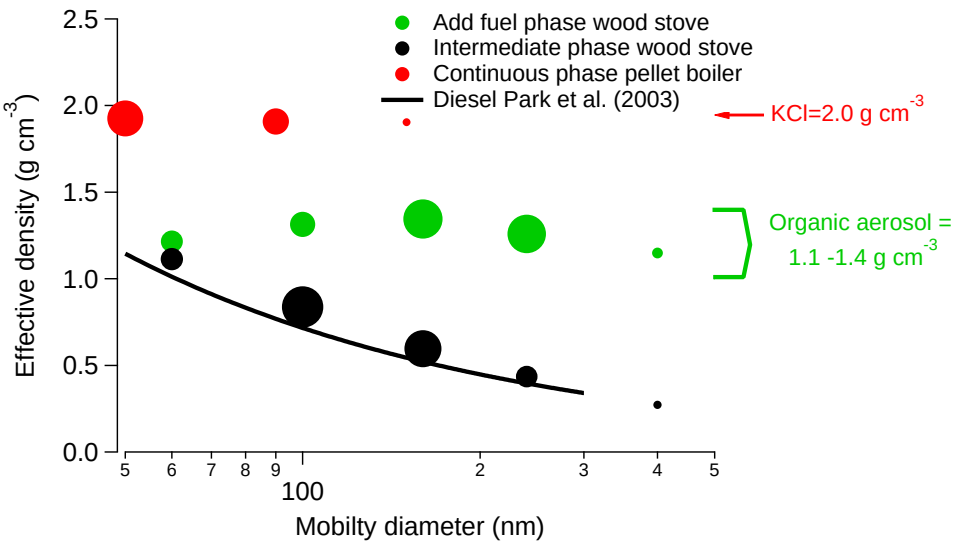

Figure 10
The mass-mobility relationships of the three main types of aerosol particles emitted from biomass combustion and a fit to mass-mobility measurements on a diesel engine presented in Park et al. (2003). The size of the cursors is proportional to the normalized number concentration at that mobility diameter within each experiment.

Boman et al. (2004) concluded that the most common alkali salts found in inorganic aerosol from pellet combustion were KCl (ρ= 2.0 g cm^{-3}) and K_2SO_4 (ρ= 2.7 g cm^{-3}). The measured value of ρ_{eff}^{I} = 1.9 g cm^{-3} is an indication that inorganic ash particles are not entirely spherical, since the effective density becomes lower than the material density with increasing deviation from spherical shapes. The aerosols emitted from the add fuel phase have an effective density similar to the bulk density of oxidized organic aerosol. In Figure 8, the highest emission factor of organic aerosol during the combustion cycle is detected during the add fuel phase. This has also been shown in Heringa et al. (2012). This is consistent with TEM analysis that shows spherical particles similar to organic "tar balls".

The soot-dominated aerosol from the intermediate phase has an effective density which is similar to or slightly higher than that of diesel soot. The mass mobility exponent for the particles emitted from the intermediate phase is 2.24, which is within the range of what is typically reported for other types of soot. The slightly higher effective density compared to diesel soot may be due to different structures of the soot agglomerates or that there is a thicker layer of organic coating on the soot from biomass combustion, which makes the particles slightly more compact in shape.

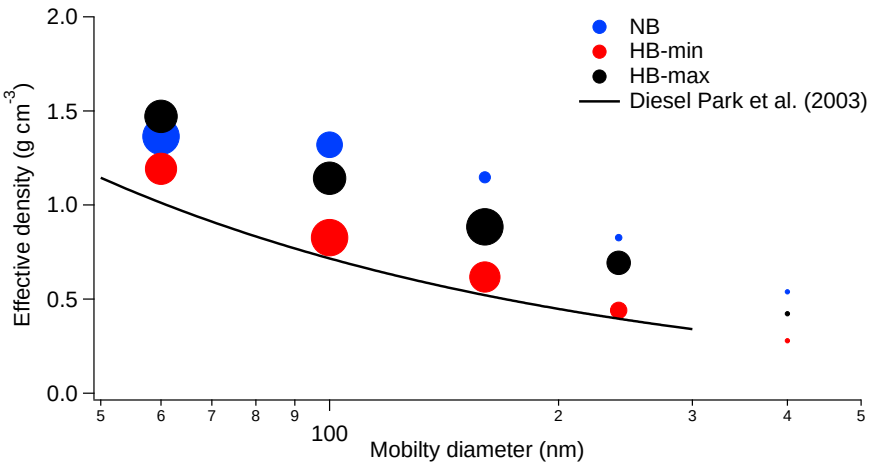

Figure 11
The effective density from complete cycles of wood combustion, at three different operation modes, nominal burn rate (NB), high burn rate-min (HB-min) and high burn rate-max (HB-max) and a fit to mass mobility measurements on emissions from a diesel engine presented in (Park et al., 2003). The size of the cursors is proportional to the number concentration at that mobility diameter within each experiment..

Figure 11 shows the mass mobility relationship of the aerosol from three complete cycles of wood log combustion operated at different combustion modes. The aerosol from the nominal burn rate cycle is dominated by smaller particles with an effective density of about 1.4 g cm^{-3}. A similar density was reported for particles from a late part of the burn about phase in Leskinen et al. (2014). The density for the larger sizes is decreasing, showing the same trend as agglomerated particles, though the effective density is considerably higher than that of diesel soot. The aerosol from the high burn rate-min experiment was the least compact of the three and had effective densities only slightly higher than for diesel soot. The mass-mobility relationship of the high burn rate-max aerosol in Figure 11 shows that the effective density is significantly higher than that of diesel soot for all mobility diameters.

Volatile mass fractions were measured with the DMA-TD-APM as described in more detail in Paper III. From these it was estimated that the organic mass fractions increased in the following order: HB-min, HB-max and NB. The highest amount of coating is found in the nominal burn rate experiment, and might be explained by organic pyrolysis products that are not degraded in the combustion, also the mass fraction of alkali salts may be highest during NB. This is consistent with soot agglomerates that for the larger sizes are more compact than diesel soot agglomerates.

In the high burn rate-max experiment there is also a relatively high degree of coating on the soot particles. A possible explanation is that the coating to some

extent is composed by PAHs, as shown in Figure 8 and in other publications such as Orasche et al. (2013). The PAH emissions increases severely for higher burn rates and overloaded combustion beds.

Mass size distributions of biomass combustion aerosol

The mass size distribution as a function of mobility diameter from a combination of scanning mobility particle sizer (SMPS) and DMA-APM data is shown in Figure 12a. The distribution of inorganic ash particles from optimal pellet combustion peaks at about 90 nm, which is to be expected (Torvela et al., 2014). The organic aerosol from the add fuel phase has a wider mass distribution which peaks around 300 nm. The organic particles from the add fuel phase of wood log combustion have been proven to be nearly spherical. The mass distribution of the soot dominated aerosol has a similar shape as the distribution of organic aerosol and peaks at almost 300 nm and most of the mass is captured within the measurement range of the SMPS.

The mass size distribution as a function of vacuum aerodynamic diameter from SP-AMS measurements is shown in Figure 12b. The curve representing inorganic ash particles is shifted to the right and the distribution peaks at ~250 nm, having a similar shape as the inorganic ash (blue) curve in Figure 12a. The curve representing organic aerosol (green) is rather wide. It is shifted slightly to the right compared to the corresponding curve in Figure 12a. The curve representing soot particles (black) peaks at a vacuum aerodynamic diameter of about 120 nm, which is significantly lower than the corresponding curve in Figure 12a.

DeCarlo et al. (2004) derived a relationship between the mobility equivalent diameter (d_{me}) and vacuum aerodynamic diameter (d_{va}) (Equation 6), using another type of effective density ρ_{eff}^{III} (where ρ_0 is unity density). If an assumption is made that ρ_{eff}^{III} is equal to ρ_{eff}^{I} in Equation 2, the mass distribution from SMPS-DMA-APM could be described as a function of vacuum aerodynamic diameter by multiplying the mobility diameter vector with the size resolved effective density. Applying the aforementioned method on the distribution described in Figure 12a gives a qualitative explanation of the rather large differences between the mass size distributions from the two approaches. However, some uncertainties remains (for example the difference in peak size for the inorganic ash case is slightly larger than the expected factor of 1.9), these may prescribed to uncertainties in the calibration of the instruments, the orientation of large soot agglomerates in the two instruments and different flow regimes (transition vs. free molecular regime).

$$d_{va} = \frac{\rho_{eff}^{III}}{\rho_0} d_{me} \qquad (6)$$

The mass-mobility relationship obtained from DMA-APM measurements enables computation of mass size distributions as a function of mobility diameter, which could be useful for lung dose estimations since the deposition mechanisms can be described by the mobility diameter (Muala et al., 2014). Converting the mass size distribution to vacuum aerodynamic diameter enables a comparison between two measurements techniques that uses different measurement principles for the determination of size and mass.

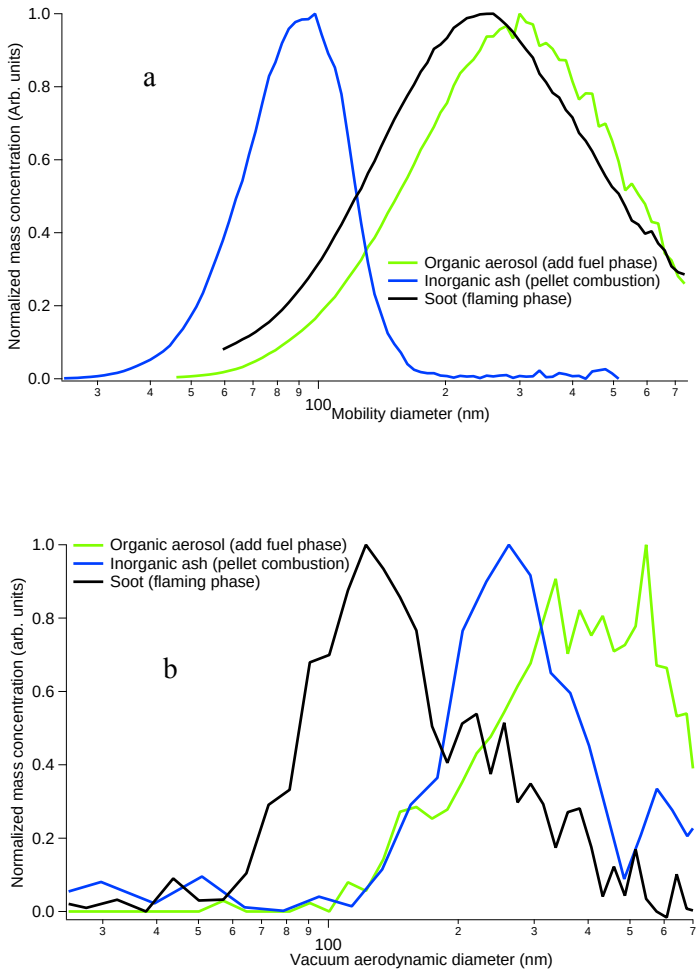

Figure 12
Normalized mass size determined from (a) number size distributions (SMPS) combined with particle effective densities (DMA+APM) as a function of mobility diameter, and (b) SP-AMS as a function of vacuum aerodynamic diameter. The curves represents organic aerosol (green), inorganic ash (blue) and soot dominated aerosol (black).

5.4 The effect of aging on chemical composition and toxicity of biomass combustion emissions – Paper IV

It is reasonable to believe that the toxicological properties of an aerosol changes with atmospheric transformation. This has also have been indicated in a study by Jalava et al. (2006), where long-range transport particles gave different toxicological responses than freshly emitted particles. In Paper IV we aimed to study the changes in toxicological responses and chemical composition due to ozone initiated aging of biomass combustion aerosol. Ozone initiated aging is relevant for biomass combustion aerosol since this type of combustion is a common source of domestic heating during winter months in the northern parts of the world, where the solar irradiation is low. Samples of fresh and aged particles emitted from two combustion modes in the wood log stove- nominal combustion (NOM) and hot air starved combustion (HAS) - were used in the cell study.

As previously discussed, PAHs are likely to be important mediators of aerosol toxicity, so portions of the particulate samples were analyzed for PAHs. The fraction of PAHs was four times higher for the hot air starved combustion compared to the nominal combustion case. PAHs are reactive (Tsapakis and Stephanou, 2003) and it is likely that they can be transformed during ozone-initiated aging of biomass combustion aerosol. Figure 13 shows the relative concentration of PAHs in the collected particle sample from the fresh and aged aerosol in the hot air starved combustion samples. The concentration of the PAHs measured is generally decreasing in the aged sample.

The lower relative PAH concentration in the aged HAS aerosol sample compared to the fresh sample is primarily due to chemical degradation of the PAHs due to ozone initiated aging. There is a trend in Figure 13 that the PAHs with the highest ozone reactivity decreases more. This is supported by a recent publication by Bruns et al. (2014), who studied changes in the chemical composition of wood smoke due to aging, where they found a significant decrease in the PAH concentration. They also found an increase in oxygenated reaction products, mostly small PAHs after aging. Previous studies (Shiraiwa et al., 2012) have also found that PAHs on particle surfaces can react with ozone and form secondary oxygenated reaction products.

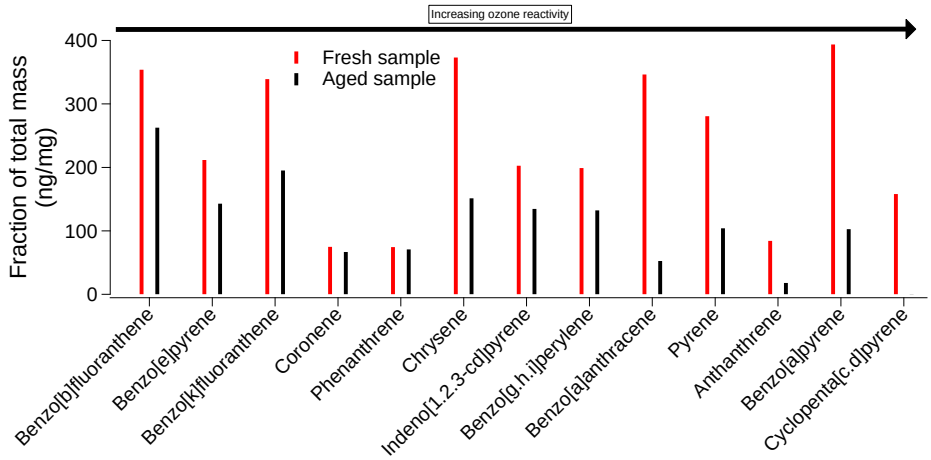

Figure 13
The relative concentration of particle phase PAHs from fresh and aged hot air starved aerosol, ordered from left to right according to their increasing ozone reactivity (Tsapakis and Stephanou, 2003).

Table 5
A summary of the most important toxicological results from the study presented in Paper IV. The toxicological study as a whole is presented in Figures 3-6 in that paper. The number of doses that show a significant difference are given in parentheses.

Toxicological test	**Fresh HAS compared to fresh NOM (number of significant differences)**	**Aged HAS compared to aged NOM (number of significant differences)**	**Aging of the HAS aerosol (number of significant differences)**
Cell death	Increase for the higher doses (3)	Increase for the higher doses (2)	Slight increase for the higher doses (1)
TNF-α	Decrease for all doses (4)	Decrease for all doses (4)	All doses at or below the control level (0)
MIP-2	No trend in dose response (2)	Significantly decreased for the highest dose (1)	Similar results (1)
Genotoxicity	No significant difference for the three lowest doses, no response was detected for the highest dose of HAS aerosol (0)	For the second highest dose there is a two-fold increase (3)	The genotoxicity increased strongly for the aged sample at the second highest dose; no response was detected for the highest dose (1)

Table 5 presents a summary of the most important results from the toxicological study in Paper IV. The results from the toxicological study generally showed an increasing response for increasing dose, except for the highest doses of fresh and aged hot air starved aerosol, where the cell death was very high. The difference due to combustion conditions showed up most clearly in the cell viability tests, where the hot air starved aerosol induces more cell death (at least for the higher doses), which is consistent with previous studies (Tapanainen et al., 2011; Jalava et al., 2012). The production of markers for tumor necrosis and macrophage inflammation is generally similar or lower for the hot air starved samples compared to the samples from nominal combustion, which would indicate that the more complete nominal combustion would induce a stronger inflammatory response.

There was a trend towards a decrease in viability for the cells exposed to the aged HAS sample compared to the cells exposed to fresh HAS sample for all doses, although only statistically significant at one dose. The genotoxicity was several times higher for the second highest dose of aged HAS compared to the fresh sample. The cells exposed to the highest dose of both fresh and aged HAS gave no response, probably due to high cell death.

DNA damage (genotoxicity) has been associated with exposure to particle samples with high PAH content (Tapanainen et al., 2011). The highest genotoxic response was induced by an aged sample from the hot air starved combustion experiment. The response was more than twice as high for the corresponding fresh sample, even though the relative fraction of PAHs was lower in the aged sample. It is likely that the PAHs had undergone degradation due to aging and have formed oxygenated (Bruns et al., 2014) and nitrated species. Oxy-PAHs can reduce oxygen to reactive oxygen species, which can induce DNA damage (Shiraiwa et al., 2012) and nitro-PAHs have high mutagenic ability (FinlaysonPitts and Pitts, 1997). There is a clear need for more studies on the health effects of degraded PAHs in particular and the toxic potential of aged aerosol in general.

5.5 Mass-mobility relationship and mixing state of urban aerosol – Paper V

Urban measurements of the mass mobility relationship

In order to determine the mixing status and particle properties of urban aerosol, a measurement campaign monitoring the air close to a busy street in central Copenhagen was performed. The DMA-APM system was deployed for roughly a month and sampled simultaneously as an SP-AMS and an SMPS. Particles were

also collected on substrates for TEM analysis during selected episodes. The long time horizon and relatively slow changes in particle properties allowed us to use high mass resolution and a wide sampling span with the DMA-APM. The same setup was placed in the rural background station at Vavihill (Tunved et al., 2003) during the same period the following year. The DMA-APM data were analyzed using the *MATLAB* program described in section 4.1, which fitted two normal distributions to the spectra.

To further investigate the influence of air mass origin on the aerosol mixing state in Copenhagen, the DMA-APM data from the measurement campaign was divided into two periods, defined from different air mass origins (Figure 14). The *Hysplit* trajectory model(Draxler and Hess, 1997) was used to derive the air mass origin. Period I had winds coming from west/northwest, thus from the Atlantic Ocean and period II had winds coming from the southeast/east/northeast, thus from continental Europe, Scandinavia and Russia.

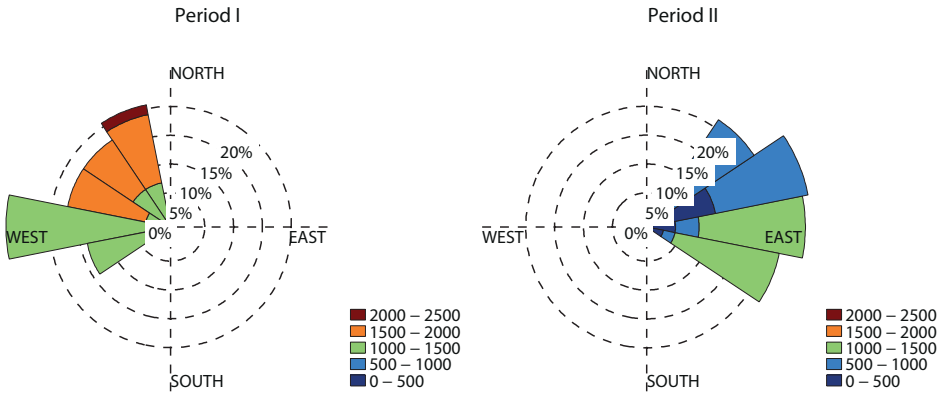

Figure 14
Air mass origins derived from *Hysplit* (Draxler and Hess, 1997) for the two periods. The color coding represents the distance to the air mass origin while the radius of the slices represents the fraction of trajectories placed in that direction.

Particles with two different types of mass-mobility relationships were observed during the measurement campaign: 1) less compact particles with an effective density that decreased with increasing mobility diameter and 2) more compact particles where the effective density was almost constant for all mobility diameters.

The measurement episodes were sorted according to the wind direction into two periods. The effective density spectra from period I was dominated by the less massive particles with low mass per particles and effective density at a given

mobility diameter (Figure 15). The effective density was decreasing with increasing particles size in a way that is typical for soot particles. The effective density spectra from period II with easterly winds was typically bimodal, which implies that the aerosol was externally mixed containing particles of two different types with two different effective densities.

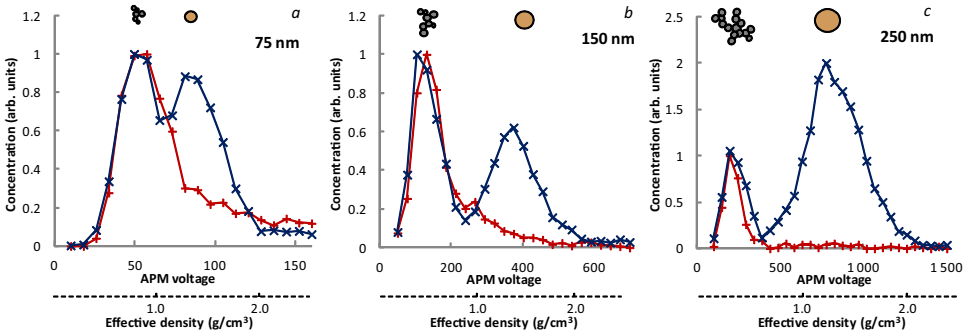

Figure 15
Typical DMA-APM voltage spectra for three mobility diameters: 75 nm (a), 150 nm (b) and 250 nm (c). The red curve represents period I and the blue curve period II. The corresponding effective density is given as an extra x-axis.

Comparing the effective density spectra from the two periods in Figure 15, it is evident that the soot mode, which is apparent in both cases, is not significantly shifted between the periods (i.e. the effective density of the soot particles are similar). The second mode which was prevalent during period II, had an effective density of 1.4 g cm^{-3}. Particles with similar density were also found at the background station Vavihill in the measurement campaign the following year. The particles from this second mode are interpreted to be long-range transport particles that consist of organic aerosol and salts such as ammonium nitrate and ammonium sulfate.

Figure 16b shows the particle number fraction of soot particles as a function of mobility diameter. The soot number fraction for the whole measurement campaign was about 50% and there was not an increasing or decreasing trend with increasing particle size. For period I, where winds had a westerly origin, the number fraction of soot aerosol increased with increasing particle size and almost 100% of the largest particles were soot. The opposite trend was seen for period II, where the number fraction decreased with increasing mobility diameter and only about 20% of the largest particles were soot.

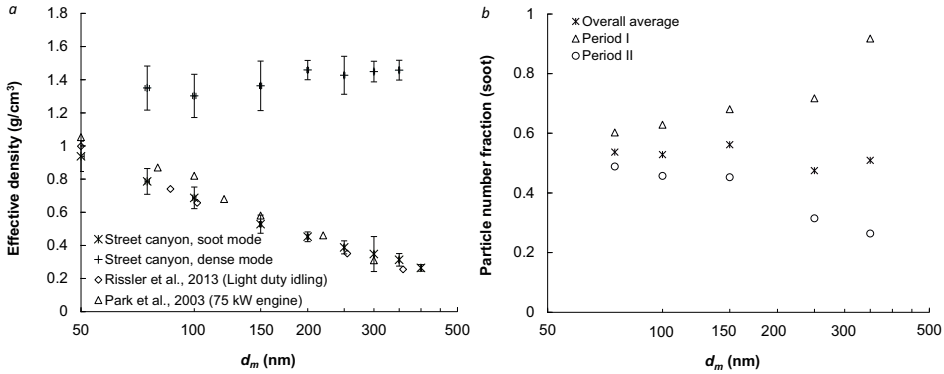

Figure 16
The average effective density (a), the errorbars are one standard deviation. The effective densities from diesel soot experiments in Rissler et al. (2013) (light duty vehicle) and Park et al. (2003) (75 kW engine) are also plotted. (b) the number fraction of aggregated particles during the urban campaign.

The mass-mobility relationship of the soot sampled in Copenhagen was compared to DMA-APM measurements of diesel soot presented in Rissler et al., (2013), where the same DMA-APM setup was used and Park et al. (2003) (Figure 16a). The average mass-mobility exponent in the Copenhagen study was 2.42. The mass mobility exponent for soot particles in Rissler et al. (2013) were 2.27 for light duty vehicles (idling) and 2.38 for heavy duty vehicles (transient) (not in the figure). This suggests that diesel soot generated in laboratories shares to a high extent the same physical characteristics as the soot found in urban environments.

5.6 Laboratory experiments on aging of diesel soot

Smog chamber experiments were performed where SOA formed from the photo-oxidation of light aromatics (a mixture of toluene and m-xylene) was condensed on diesel soot particles in order to study the effect of the atmospheric transformation on the diesel soot properties. The same smog chamber setup as described in Paper I was used. Measurements using the DMA-APM technique were performed before the photo-oxidation started and throughout the experiment. The DMA was set at a fixed voltage and with the APM the mass was measured at each mobility diameter bypass and through a thermodenuder (300 °C) in adjacent runs. The mass growth factor was defined as the ratio between the mass of the particles bypassing the thermodenuder ($mass_{proc}$) and the mass of the particles passing through the thermodenuder ($mass_{fresh}$) for each mobility diameter.

The effective density as a function of mass growth factor is plotted in Figure 17. For fresh soot at a mass growth factor of 1, the effective densities decreased with increasing mobility diameters. The effective density values were typical for fresh diesel soot (Park et al., 2003; Rissler et al., 2013). Initially the density increased with increasing mass growth factor but eventually the effective density converged to about 1.4 g cm^{-3}, which is about the same number as previous observations of SOA density (Ng et al., 2007), assuming spherical particles.

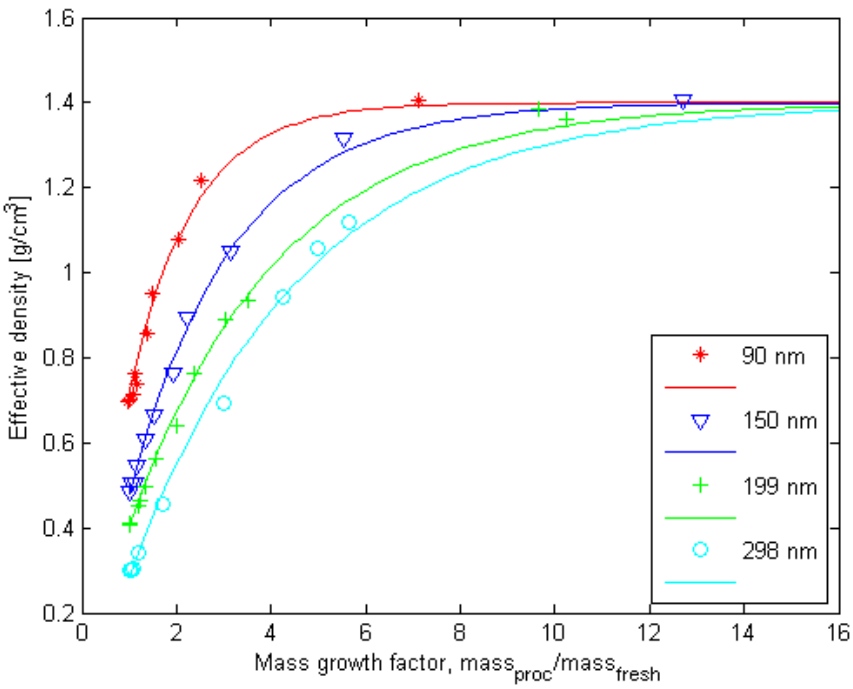

Figure 17
The effective density as a function of mass growth factor for four mobility diameters during simulated atmospheric processing of diesel soot in the smog chamber.

The effective density of the aged diesel soot converged towards the density of SOA, which is expected since a majority of the mass is SOA. Larger mobility diameters require a higher mass growth factor, i.e. more condensed mass before converging to spherical particles). That is to be expected since the larger agglomerates have a higher dynamic shape factor. Thus having a lower effective density requires more SOA mass to fill the voids in the structure. The transformation also includes restructuring of the soot core to a more compact shape (Pagels et al., 2009).

Comparison of ambient measurements and laboratory studies

Comparing the mass-mobility relationship of the soot particles measured on the street in Copenhagen with the mass-mobility relationship measured in previous laboratory studies indicates that the observations of aggregated soot particles in Copenhagen comes from nearby anthropogenic combustion sources, possibly from the same street. That is also supported by the diurnal emission pattern, Figure 5a in Paper V shows that the number fraction of soot aggregates is highest around rush hours and that the soot number fraction correlates with NO_x emissions (Figure 5b, Paper V).

The density of the long range transport particles is similar ~1.4 g cm^{-3} to the density that the aged soot particles in the laboratory study converged to. Figure 17 also shows in the laboratory experiments, that the soot mass fraction of an aged particle with a density of 1.4 g cm^{-3} is only ~10-20% of the total particle mass. The non-volatile (most probably soot) fraction of the long-range transport particles in the urban study was not possible to resolve, due to the interference with freshly emitted soot in the APM spectra. The non-volatile fraction of the long-range transport particles found at the background station varied between ~20% down to almost zero from day to day, larger particles had generally had lower mass fractions of non-volatile material. It was however not possible to resolve what number fraction of the long-range particles that had a soot core. From both laboratory studies and field measurements it is evident that only a small mass percentage of the internally mixed aged particles are soot. A substantial fraction of the soot in urban environments is freshly emitted.

6 Conclusions and outlook

6.1 Conclusions

This thesis has presented new knowledge on the characteristics of fresh and aged particles emitted from in-use combustion sources. Novel in situ techniques have been used to characterize the physical and chemical particle properties on-line.

Traditional secondary organic aerosol (SOA) precursors were responsible for up to 60% of the SOA formed from idling gasoline vehicle exhaust studied in the newly implemented smog chamber system. The vast majority of the organic aerosol produced from gasoline vehicles is secondary, even in the relatively short window of several hours of atmospheric aging studied here. Secondary organic aerosol from gasoline vehicle exhaust is likely to contribute to the aerosol in and downwind urban areas.

The emissions of particulate phase polycyclic aromatic hydrocarbons (PAHs) were almost an order of magnitude higher for high burn rate operations compared to nominal operations of a common conventional wood stove. The highest PAH emissions occurred during episodes of fast burning at hot air starved conditions, in the intermediate (flaming) combustion phase.

Three main particle types with significantly different mass-mobility relationships were found in biomass combustion emissions, consistent with spherical organic particles, soot agglomerates and compact inorganic ash particles. The particle types originated from different combustion situations. The mass-mobility relationship of full-cycle wood stove emissions was affected by combustion conditions.

Particles from less efficient combustion in the wood stove (high OA and PAHs) were a more potent inducer of cell death than particles from more complete combustion. Particles from aged less efficient combustion induced altered toxicological responses (e.g. genotoxicity) compared to fresh particles from the same combustion mode. The alterations in toxicological response were hypothesized to be caused by organic degradation products (including PAHs) formed from ozone-initiated dark processing of the combustion aerosol.

Two major types of particles with different mass-mobility relationships were observed at urban street level, and identified as soot agglomerates and compact

long range transport particles. The fraction of soot agglomerates correlated with nitrogen oxide emissions, while the long-range transport particles were to a higher extent present in polluted air masses during days of easterly winds. The soot agglomerates analyzed at street level had characteristics that were similar to those emitted from diesel engines studied in laboratory experiments.

The results presented in this thesis show that the physical, chemical and toxicological properties of carbonaceous aerosol from anthropogenic combustion are affected by source, combustion conditions and atmospheric aging. This needs to be taken into account when assessing health and climate effects of aerosol particles.

6.2 Outlook

In order to make accurate estimations of how anthropogenic combustion emissions can affect public health, more information is needed about which physical and chemical characteristics that drive the negative health effects. Hence it is important to combine human exposure and cell studies with detailed chemical and physical characterization of the aerosol.

To be able to make better predictions of the climate effects of aerosol particles, more accurate global aerosol modelling is needed. To improve global aerosol modelling, more data, such as emission factors from primary and secondary sources and the mixing state of absorbing components are needed, as well as ambient aerosol monitoring to validate the models.

Earlier recommendations on emissions reduction from small scale biomass combustion have focused on avoiding low temperature combustion due to the resulting high mass emissions of organic aerosol. There emissions are caused by high moisture content in the fuel, poorly insulated stoves, etc. The data presented in this thesis suggests that hot air starved combustion also should be avoided due to the high PAH emissions. Hot air starved combustion is best avoided by upgrading old wood stoves to modern pellet combustion techniques, though it might not be feasible to replace all existing wood stoves. Monitoring O_2 in the flue gases as an indication of PAH emission might be a cost effective way to identify potential PAH emissions from wood stoves.

The toxicity of aged biomass combustion aerosol clearly merits further investigation to improve knowledge about the health effects and toxic potential of the aerosol from various types of biomass combustion.

Finally, it should be mentioned that the conclusions are based on experiments performed on a limited number of biomass combustion appliances and vehicles. More extensive studies are needed.

Acknowledgements

First and foremost I would like to acknowledge my main supervisor Dr. Joakim Pagels, who back in 2008 recruited me to the aerosol business. Thank you for always being very encouraging and inspiring but at the same time challenging and demanding, in an effort to bring the best out of me. Thank you for always having time for discussions and mentoring. I am especially grateful for the long hours you have spent lately helping me with improving this thesis.

I also want to thank my co-supervisor Dr. Anders Gudmundsson for always being positive, encouraging and supporting during my time as a doctoral student, and for making sure that the aerosol laboratory is a good working environment with a creative atmosphere.

I want to thank my co-supervisor Dr. Jenny Rissler for your support, mentorship and for teaching me a lot about soot particles and the APM.

I want to thank my former main supervisor Prof. Mats Bohgard for encouraging high academic standards and for being a great leader for the aerosol group at EAT while letting other people shine.

I want to thank Prof. Erik Swietlicki for your time as co-supervisor and for being a true motivator; I will bring with me your words: “If something would have been easy, someone else would already have done it”.

Thank you Dr. Christina Isaxon, it has been a pleasure sharing office with you for five years. We have had many interesting discussions about science and other stuff and tested a lot of ideas and hypothesis on each other, which I believe in the end have improved our abilities as researchers.

I want to acknowledge Axel Eriksson, for your excellent work with the AMS in experimental campaigns and analyzing the data, you have had an important role in all of the work presented in this thesis. I also want to thank you for good company during measurement campaigns and journeys and for teaching me a thing or two about physics.

I also want to thank my fellow doctoral students at EAT Patrik Nilsson, Christian Svensson and Jonas Jakobsson for good company, fruitful lunch discussions and for sharing fun moments during travelling and while working in the laboratory.

I would like to acknowledge Dr. Pontus Roldin and Jonatan Carlsson for support and valuable input during the smog chamber campaign and writing of Paper I.

Dr. Christoffer Boman, Robin Nyström and Robert Lindgren from Umeå University for welcoming us to your city and for good teamwork during the different biomass combustion campaigns. Prof. Maija-Riitta Hirvonen and Dr. Oskari Uski from Finnish Institute for Health and Welfare in Kuopio for an excellent interdisciplinary collaboration working with Paper IV.

I would like to thank all of the former and present doctoral students and senior staff at the aerosol groups of EAT and Nuclear Physics for creating a great working atmosphere and a dynamic research climate, and for many memories from conferences and journeys, it has been a pleasure to know you all!

I also want to thank all of the administrative personnel at the Department of Design Sciences for always being very helpful and making life easy for all the scientists. A special thanks to Eileen Deaner for doing such a rigorous job with language editing my thesis and papers, you have really improved my work, and to Karin Öhrvik, for always being so helpful with all kinds of administrative problems, there isn't anything worth knowing about university administration that you don't know of.

I want to thank my parents Ann-Sofi and Anders for all the support throughout the years, for always stressing the importance of education and for teaching me not to be overly impressed with things, and my sister Lovisa, for being a true friend while we still always compete against each other.

Last but definitely not least I would like to thank my wife Anna and our child Sigrid, you mean everything to me and every day you remind me that there is a lot more to life than work.

References

Aiken, A. C., Decarlo, P. F., Kroll, J. H., Worsnop, D. R., Huffman, J. A., Docherty, K. S., Ulbrich, I. M., Mohr, C., Kimmel, J. R., Sueper, D., Sun, Y., Zhang, Q., Trimborn, A., Northway, M., Ziemann, P. J., Canagaratna, M. R., Onasch, T. B., Alfarra, M. R., Prevot, A. S. H., Dommen, J., Duplissy, J., Metzger, A., Baltensperger, U. and Jimenez, J. L. (2008). *O/C and OM/OC ratios of primary, secondary, and ambient organic aerosols with high-resolution time-of-flight aerosol mass spectrometry*. Environ Sci Technol **42**(12): 4478-4485.

Bahreini, R., Middlebrook, A. M., de Gouw, J. A., Warneke, C., Trainer, M., Brock, C. A., Stark, H., Brown, S. S., Dube, W. P., Gilman, J. B., Hall, K., Holloway, J. S., Kuster, W. C., Perring, A. E., Prevot, A. S. H., Schwarz, J. P., Spackman, J. R., Szidat, S., Wagner, N. L., Weber, R. J., Zotter, P. and Parrish, D. D. (2012). *Gasoline emissions dominate over diesel in formation of secondary organic aerosol mass*. Geophys Res Lett **39**.

Barregard, L., Sallsten, G., Gustafson, P., Andersson, L., Johansson, L., Basu, S. and Stigendal, L. (2006). *Experimental exposure to wood-smoke particles in healthy humans: Effects on markers of inflammation, coagulation, and lipid peroxidation*. Inhal Toxicol **18**(11): 845-853.

Benbrahim-Tallaa, L., Baan, R. A., Grosse, Y., Lauby-Secretan, B., El Ghissassi, F., Bouvard, V., Guha, N., Loomis, D. and Straif, K. (2012). *Carcinogenicity of diesel-engine and gasoline-engine exhausts and some nitroarenes*. The lancet oncology **13**(7): 663-664.

Blanco, G., Gerlagh, R., Suh, S., Barrett, J., de Coninck, H. C., Diaz Morejon, C. F., Mathur, R., Nakicenovic, N., Ofosu Ahenkora, A., Pan, J., Pathak, H., Rice, J., Richels, R., Smith, S. J., Stern, D. I., Toth, F. L. and Zhou, P., 2014: *Mitigation of Climate Change. Contribution of Working Group III to the Fifth Assessment Report of the Intergovernmental Panel on Climate Change* [O. Edenhofer, R. Pichs-Madruga, Y. Sokona, E. Farahani, S. Kadner, K. Seyboth, A. Adler, I. Baum, S. Brunner, P. Eickemeier, B. Kriemann, J. Savolainen, S. S. Schlömer, C. von Stechow, T. Zwickel and J. C. Minx (eds.)]. C. U. Press, Cambridge, United Kingdom and New York, NY, USA.

Boman, C., Nordin, A., Bostrom, D. and Ohman, M. (2004). *Characterization of inorganic particulate matter from residential combustion of pelletized biomass fuels*. Energ Fuel **18**(2): 338-348.

Boman, C., Pettersson, E., Westerholm, R., Bostrom, D. and Nordin, A. (2011). *Stove Performance and Emission Characteristics in Residential Wood Log and Pellet Combustion, Part 1: Pellet Stoves*. Energ Fuel **25**: 307-314.

Bond, T. C., Doherty, S. J., Fahey, D. W., Forster, P. M., Berntsen, T., DeAngelo, B. J., Flanner, M. G., Ghan, S., Karcher, B., Koch, D., Kinne, S., Kondo, Y., Quinn, P. K., Sarofim, M. C., Schultz, M. G., Schulz, M., Venkataraman, C., Zhang, H., Zhang, S., Bellouin, N., Guttikunda, S. K., Hopke, P. K., Jacobson, M. Z., Kaiser, J. W., Klimont, Z., Lohmann, U., Schwarz, J. P., Shindell, D., Storelvmo, T., Warren, S. G. and Zender, C. S. (2013). *Bounding the role of black carbon in the climate system: A scientific assessment*. J Geophys Res-Atmos **118**(11): 5380-5552.

Brandt, C., Kunde, R., Dobmeier, B., Schnelle-Kreis, J., Orasche, J., Schmoeckel, G., Diemer, J., Zimmermann, R. and Gaderer, M. (2011). *Ambient PM10 concentrations from wood combustion - Emission modeling and dispersion calculation for the city area of Augsburg, Germany*. Atmos Environ **45**(20): 3466-3474.

Brook, R. D., Rajagopalan, S., Pope, C. A., Brook, J. R., Bhatnagar, A., Diez-Roux, A. V., Holguin, F., Hong, Y. L., Luepker, R. V., Mittleman, M. A., Peters, A., Siscovick, D., Smith, S. C., Whitsel, L., Kaufman, J. D., Epidemiol, A. H. A. C., Dis, C. K. C. and Metab, C. N. P. A. (2010). *Particulate Matter Air Pollution and Cardiovascular Disease An Update to the Scientific Statement From the American Heart Association*. Circulation **121**(21): 2331-2378.

Bruns, E. A., Krapf, M., Orasche, J., Huang, Y., Zimmermann, R., Drinovec, L., Močnik, G., El-Haddad, I., Slowik, J. G., Dommen, J., Baltensperger, U. and Prévôt, A. S. H. (2014). *Characterization of primary and secondary wood combustion products generated under different burner loads*. Atmos. Chem. Phys. Discuss. **14**(19): 26041-26083.

Chen, Y. and Bond, T. C. (2010). *Light absorption by organic carbon from wood combustion*. Atmos Chem Phys **10**(4): 1773-1787.

Chirico, R., DeCarlo, P. F., Heringa, M. F., Tritscher, T., Richter, R., Prevot, A. S. H., Dommen, J., Weingartner, E., Wehrle, G., Gysel, M., Laborde, M. and Baltensperger, U. (2010). *Impact of aftertreatment devices on primary emissions and secondary organic aerosol formation potential from in-use diesel vehicles: results from smog chamber experiments*. Atmos Chem Phys **10**(23): 11545-11563.

Chung, C. E., Lee, K. and Muller, D. (2012). *Effect of internal mixture on black carbon radiative forcing*. Tellus B **64**: 1-13.

Cocker, D. R., Flagan, R. C. and Seinfeld, J. H. (2001). *State-of-the-art chamber facility for studying atmospheric aerosol chemistry*. Environ Sci Technol **35**(12): 2594-2601.

DeCarlo, P. F., Kimmel, J. R., Trimborn, A., Northway, M. J., Jayne, J. T., Aiken, A. C., Gonin, M., Fuhrer, K., Horvath, T., Docherty, K. S., Worsnop, D. R. and Jimenez, J. L. (2006). *Field-deployable, high-resolution, time-of-flight aerosol mass spectrometer*. Anal Chem **78**(24): 8281-8289.

DeCarlo, P. F., Slowik, J. G., Worsnop, D. R., Davidovits, P. and Jimenez, J. L. (2004). *Particle morphology and density characterization by combined mobility and aerodynamic diameter measurements. Part 1: Theory*. Aerosol Sci Tech **38**(12): 1185-1205.

Dockery, D. W., Pope, C. A., Xu, X. P., Spengler, J. D., Ware, J. H., Fay, M. E., Ferris, B. G. and Speizer, F. E. (1993). *An Association between Air-Pollution and Mortality in 6 United-States Cities*. New Engl J Med **329**(24): 1753-1759.

Donahue, N. M., Robinson, A. L., Stanier, C. O. and Pandis, S. N. (2006). *Coupled partitioning, dilution, and chemical aging of semivolatile organics*. Environ Sci Technol **40**(8): 2635-2643.

Draxler, R. R. and Hess, G. (1997). *Description of the HYSPLIT4 modeling system*.

Dzepina, K., Arey, J., Marr, L. C., Worsnop, D. R., Salcedo, D., Zhang, Q., Onasch, T. B., Molina, L. T., Molina, M. J. and Jimenez, J. L. (2007). *Detection of particle-phase polycyclic aromatic hydrocarbons in Mexico City using an aerosol mass spectrometer*. Int J Mass Spectrom **263**(2-3): 152-170.

EEB. (2014). *Air & domestic heating*. Retrieved 12th dec, 2014, from http://www.eeb.org/EEB/?LinkServID=2A5A923A-5056-B741-DB09EE1D757AC04C.

Elsasser, M., Busch, C., Orasche, J., Schon, C., Hartmann, H., Schnelle-Kreis, J. and Zimmermann, R. (2013). Dynamic Changes of the Aerosol Composition and Concentration during Different Burning Phases of Wood Combustion. Energ Fuel 27(8): 4959-4968.

Emery, M. (2005). Theoretical analysis of data from DMA-APM system. MsC Thesis Mechanical Engineering Univ. of Minnesota: 63.

EUR-Lex. (2014). EUR-Lex data base. Retrieved 12th dec, 2014, from http://eur-lex.europa.eu/browse/summaries.html.

Faustini, A., Rapp, R. and Forastiere, F. (2014). *Nitrogen dioxide and mortality: review and meta-analysis of long-term studies*. Eur Respir J **44**(3): 744-753.

FinlaysonPitts, B. J. and Pitts, J. N. (1997). *Tropospheric air pollution: Ozone, airborne toxics, polycyclic aromatic hydrocarbons, and particles*. Science **276**(5315): 1045-1052.

Fountoukis, C., Butler, T., Lawrence, M., Denier van der Gon, H., Visschedijk, A., Charalampidis, P., Pilinis, C. and Pandis, S. (2014). *Impacts of controlling biomass burning emissions on wintertime carbonaceous aerosol in Europe*. Atmos Environ **87**: 175-182.

Gaschen, A., Lang, D., Kalberer, M., Savi, M., Geiser, T., Gazdhar, A., Lehr, C. M., Bur, M., Dommen, J., Baltensperger, U. and Geiser, M. (2010). *Cellular Responses after Exposure of Lung Cell Cultures to Secondary Organic Aerosol Particles*. Environ Sci Technol **44**(4): 1424-1430.

Gentner, D. R., Isaacman, G., Worton, D. R., Chan, A. W. H., Dallmann, T. R., Davis, L., Liu, S., Day, D. A., Russell, L. M., Wilson, K. R., Weber, R., Guha, A., Harley, R. A. and Goldstein, A. H. (2012). *Elucidating secondary organic aerosol from diesel and gasoline vehicles through detailed characterization of organic carbon emissions*. Proceedings of the National Academy of Sciences **109**(45): 18318-18323.

Glassman, I. and Yetter, R. A. (2008). *Combustion*, Academic Press Inc

Hallquist, M., Wenger, J. C., Baltensperger, U., Rudich, Y., Simpson, D., Claeys, M., Dommen, J., Donahue, N. M., George, C., Goldstein, A. H., Hamilton, J. F., Herrmann, H., Hoffmann, T., Iinuma, Y., Jang, M., Jenkin, M. E., Jimenez, J. L., Kiendler-Scharr, A., Maenhaut, W., McFiggans, G., Mentel, T. F., Monod, A., Prevot, A. S. H., Seinfeld, J. H., Surratt, J. D., Szmigielski, R. and Wildt, J. (2009). *The formation, properties and impact of secondary organic aerosol: current and emerging issues*. Atmos Chem Phys **9**(14): 5155-5236.

Heringa, M. F., DeCarlo, P. F., Chirico, R., Lauber, A., Doberer, A., Good, J., Nussbaumer, T., Keller, A., Burtscher, H., Richard, A., Miljevic, B., Prevot, A. S. H. and Baltensperger, U. (2012). *Time-Resolved Characterization of Primary Emissions from Residential Wood Combustion Appliances*. Environ Sci Technol **46**(20): 11418-11425.

Hildebrandt, L., Donahue, N. M. and Pandis, S. N. (2009). *High formation of secondary organic aerosol from the photo-oxidation of toluene*. Atmos Chem Phys **9**(9): 2973-2986.

Hoek, G., Brunekreef, B., Goldbohm, S., Fischer, P. and van den Brandt, P. A. (2002). *Association between mortality and indicators of traffic-related air pollution in the Netherlands: a cohort study*. Lancet **360**(9341): 1203-1209.

IARC (2010). *IARC MONOGRAPHS ON THE EVALUATION OF CARCINOGENIC RISKS TO HUMANS*. Iarc Monographs on the Evaluation of Carcinogenic Risks to Humans, Vol 95: Household Use of Solid Fuels and High-Temperature Frying. Geneva, World Health Organization. **95:** 9-38.

Jalava, P., Salonen, R. O., Halinen, A. I., Sillanpaa, M., Sandell, E. and Hirvonen, M. R. (2005). *Effects of sample preparation on chemistry, cytotoxicity, and inflammatory responses induced by air particulate matter*. Inhal Toxicol **17**(2): 107-117.

Jalava, P. I., Happo, M. S., Kelz, J., Brunner, T., Hakulinen, P., Maki-Paakkanen, J., Hukkanen, A., Jokiniemi, J., Obernberger, I. and Hirvonen, M. R. (2012). *In vitro toxicological characterization of particulate emissions from residential biomass heating systems based on old and new technologies*. Atmos Environ **50**: 24-35.

Jalava, P. I., Salonen, R. O., Halinen, A. I., Penttinen, P., Pennanen, A. S., Sillanpaa, M., Sandell, E., Hillamo, R. and Hirvonen, M. R. (2006). *In vitro inflammatory and cytotoxic effects of size-segregated particulate samples collected during long-range transport of wildfire smoke to Helsinki*. Toxicol Appl Pharm **215**(3): 341-353.

Jalava, P. I., Salonen, R. O., Nuutinen, K., Pennanen, A. S., Happo, M. S., Tissari, J., Frey, A., Hillamo, R., Jokiniemi, J. and Hirvonen, M. R. (2010). *Effect of combustion condition on cytotoxic and inflammatory activity of residential wood combustion particles*. Atmos Environ **44**(13): 1691-1698.

Kittelson, D. B. (1998). *Engines and nanoparticles: A review*. J Aerosol Sci **29**(5-6): 575-588.

Kocbach-Bølling, A., Pagels, J., Yttri, K. E., Barregard, L., Sallsten, G., Schwarze, P. E. and Boman, C. (2009). *Health effects of residential wood smoke particles: the importance of combustion conditions and physicochemical particle properties*. Part Fibre Toxicol **6**.

Krecl, P., Larsson, E. H., Strom, J. and Johansson, C. (2008). *Contribution of residential wood combustion and other sources to hourly winter aerosol in Northern Sweden determined by positive matrix factorization*. Atmos Chem Phys **8**(13): 3639-3653.

Kunzi, L., Mertes, P., Schneider, S., Jeannet, N., Menzi, C., Dommen, J., Baltensperger, U., Prevot, A. S. H., Salathe, M., Kalberer, M. and Geiser, M. (2013). *Responses of lung cells to realistic exposure of primary and aged carbonaceous aerosols*. Atmos Environ **68**: 143-150.

Lack, D. A., Langridge, J. M., Bahreini, R., Cappa, C. D., Middlebrook, A. M. and Schwarz, J. P. (2012). *Brown carbon and internal mixing in biomass burning particles*. P Natl Acad Sci USA **109**(37): 14802-14807.

Legreid, G., Reimann, S., Steinbacher, M., Staehelin, J., Young, D. and Stemmler, K. (2007). *Measurements of OVOCs and NMHCs in a swiss highway tunnel for estimation of road transport emissions*. Environ Sci Technol **41**(20): 7060-7066.

Leskinen, J., Ihalainen, M., Torvela, T., Kortelainen, M., Lamberg, H., Tiitta, P., Jakobi, G., Grigonyte, J., Joutsensaari, J. and Sippula, O. (2014). *Effective Density and Morphology of Particles Emitted from Small-Scale Combustion of Various Wood Fuels*. Environ Sci Technol.

Lighty, J. S., Veranth, J. M. and Sarofim, A. F. (2000). *Combustion aerosols: Factors governing their size and composition and implications to human health*. J Air Waste Manage **50**(9): 1565-1618.

Malik, A., Abdulhamid, H., Pagels, J., Rissler, J., Lindskog, M., Nilsson, P., Bjorklund, R., Jozsa, P., Visser, J., Spetz, A. and Sanati, M. (2011). *A Potential Soot Mass Determination Method from Resistivity Measurement of Thermophoretically Deposited Soot*. Aerosol Sci Tech **45**(2): 284-294.

Maricq, M. M. (2007). *Chemical characterization of particulate emissions from diesel engines: A review*. J Aerosol Sci **38**(11): 1079-1118.

May, A. A., Nguyen, N. T., Presto, A. A., Gordon, T. D., Lipsky, E. M., Karve, M., Gutierrez, A., Robertson, W. H., Zhang, M., Brandow, C., Chang, O., Chen, S. Y., Cicero-Fernandez, P., Dinkins, L., Fuentes, M., Huang, S. M., Ling, R., Long, J., Maddox, C., Massetti, J., McCauley, E., Miguel, A., Na, K., Ong, R., Pang, Y. B., Rieger, P., Sax, T., Truong, T., Vo, T., Chattopadhyay, S., Maldonado, H., Maricq, M. M. and Robinson, A. L. (2014). *Gas- and particle-phase primary emissions from in-use, on-road gasoline and diesel vehicles*. Atmos Environ **88**: 247-260.

McMurry, P. H. and Rader, D. J. (1985). *Aerosol Wall Losses in Electrically Charged Chambers*. Aerosol Sci Tech **4**(3): 249-268.

McMurry, P. H., Wang, X., Park, K. and Ehara, K. (2002). *The relationship between mass and mobility for atmospheric particles: A new technique for measuring particle density*. Aerosol Sci Tech **36**(2): 227-238.

Monks, P. S., Granier, C., Fuzzi, S., Stohl, A., Williams, M. L., Akimoto, H., Amann, M., Baklanov, A., Baltensperger, U., Bey, I., Blake, N., Blake, R. S., Carslaw, K., Cooper, O. R., Dentener, F., Fowler, D., Fragkou, E., Frost, G. J., Generoso, S., Ginoux, P., Grewe, V., Guenther, A., Hansson, H. C., Henne, S., Hjorth, J., Hofzumahaus, A., Huntrieser, H., Isaksen, I. S. A., Jenkin, M. E., Kaiser, J., Kanakidou, M., Klimont, Z., Kulmala, M., Laj, P., Lawrence, M. G., Lee, J. D., Liousse, C., Maione, M., McFiggans, G., Metzger, A., Mieville, A., Moussiopoulos, N., Orlando, J. J., O'Dowd, C. D., Palmer, P. I., Parrish, D. D., Petzold, A., Platt, U., Poschl, U., Prevot, A. S. H., Reeves, C. E., Reimann, S., Rudich, Y., Sellegri, K., Steinbrecher, R., Simpson, D., ten Brink, H., Theloke, J., van der Werf, G. R., Vautard, R., Vestreng, V., Vlachokostas, C. and von Glasow, R. (2009). *Atmospheric composition change - global and regional air quality*. Atmos Environ **43**(33): 5268-5350.

Muala, A., Nicklasson, H., Boman, C., Swietlicki, E., Nyström, R., Pettersson, E., Bosson, J. A., Rissler, J., Blomberg, A. and Sandström, T. (2014). *Respiratory Tract*

Deposition of Inhaled Wood Smoke Particles in Healthy Volunteers. J Aerosol Med Pulm D.

Ng, N. L., Kroll, J. H., Chan, A. W. H., Chhabra, P. S., Flagan, R. C. and Seinfeld, J. H. (2007). *Secondary organic aerosol formation from m-xylene, toluene, and benzene*. Atmos Chem Phys **7**(14): 3909-3922.

Odum, J. R., Jungkamp, T. P. W., Griffin, R. J., Forstner, H. J. L., Flagan, R. C. and Seinfeld, J. H. (1997). *Aromatics, reformulated gasoline, and atmospheric organic aerosol formation*. Environ Sci Technol **31**(7): 1890-1897.

Onasch, T. B., Trimborn, A., Fortner, E. C., Jayne, J. T., Kok, G. L., Williams, L. R., Davidovits, P. and Worsnop, D. R. (2012). *Soot Particle Aerosol Mass Spectrometer: Development, Validation, and Initial Application*. Aerosol Sci Tech **46**(7): 804-817.

Orasche, J., Schnelle-Kreis, J., Schon, C., Hartmann, H., Ruppert, H., Arteaga-Salas, J. M. and Zimmermann, R. (2013). *Comparison of Emissions from Wood Combustion. Part 2: Impact of Combustion Conditions on Emission Factors and Characteristics of Particle-Bound Organic Species and Polycyclic Aromatic Hydrocarbon (PAH)-Related Toxicological Potential*. Energ Fuel **27**(3): 1482-1491.

Orasche, J., Seidel, T., Hartmann, H., Schnelle-Kreis, J., Chow, J. C., Ruppert, H. and Zimmermann, R. (2012). *Comparison of Emissions from Wood Combustion. Part 1: Emission Factors and Characteristics from Different Small-Scale Residential Heating Appliances Considering Particulate Matter and Polycyclic Aromatic Hydrocarbon (PAH)-Related Toxicological Potential of Particle-Bound Organic Species*. Energ Fuel **26**(11): 6695-6704.

Pagels, J., Khalizov, A. F., McMurry, P. H. and Zhang, R. Y. (2009). *Processing of Soot by Controlled Sulphuric Acid and Water CondensationMass and Mobility Relationship*. Aerosol Sci Tech **43**(7): 629-640.

Park, K., Cao, F., Kittelson, D. B. and McMurry, P. H. (2003). *Relationship between particle mass and mobility for diesel exhaust particles*. Environ Sci Technol **37**(3): 577-583.

Paulsen, D., Dommen, J., Kalberer, M., Prevot, A. S. H., Richter, R., Sax, M., Steinbacher, M., Weingartner, E. and Baltensperger, U. (2005). *Secondary organic aerosol formation by irradiation of 1,3,5-trimethylbenzene-NOx-H2O in a new reaction chamber for atmospheric chemistry and physics*. Environ Sci Technol **39**(8): 2668-2678.

Pettersson, E., Boman, C., Westerholm, R., Bostrom, D. and Nordin, A. (2011). *Stove Performance and Emission Characteristics in Residential Wood Log and Pellet Combustion, Part 2: Wood Stove*. Energ Fuel **25**: 315-323.

Rissler, J., Messing, M. E., Malik, A. I., Nilsson, P. T., Nordin, E. Z., Bohgard, M., Sanati, M. and Pagels, J. H. (2013). *Effective Density Characterization of Soot Agglomerates from Various Sources and Comparison to Aggregation Theory*. Aerosol Sci Tech **47**(7): 792-805.

Robinson, A. L., Donahue, N. M., Shrivastava, M. K., Weitkamp, E. A., Sage, A. M., Grieshop, A. P., Lane, T. E., Pierce, J. R. and Pandis, S. N. (2007). *Rethinking organic aerosols: Semivolatile emissions and photochemical aging*. Science **315**(5816): 1259-1262.

Roldin, P., Eriksson, A. C., Nordin, E. Z., Hermansson, E., Mogensen, D., Rusanen, A., Boy, M., Swietlicki, E., Svenningsson, B., Zelenyuk, A. and Pagels, J. (2014). *Modelling non-equilibrium secondary organic aerosol formation and evaporation with the aerosol dynamics, gas- and particle-phase chemistry kinetic multilayer model ADCHAM*. Atmos Chem Phys **14**(15): 7953-7993.

Ruckerl, R., Schneider, A., Breitner, S., Cyrys, J. and Peters, A. (2011). *Health effects of particulate air pollution: A review of epidemiological evidence*. Inhal Toxicol **23**(10): 555-592.

Ruusunen, J., Tapanainen, M., Sippula, O., Jalava, P. I., Lamberg, H., Nuutinen, K., Tissari, J., Ihalainen, M., Kuuspalo, K., Maki-Paakkanen, J., Hakulinen, P., Pennanen, A., Teinila, K., Makkonen, U., Salonen, R. O., Hillamo, R., Hirvonen, M. R. and Jokiniemi, J. (2011). *A novel particle sampling system for physico-chemical and toxicological characterization of emissions*. Anal Bioanal Chem **401**(10): 3183-3195.

Sakurai, H., Tobias, H. J., Park, K., Zarling, D., Docherty, K. S., Kittelson, D. B., McMurry, P. H. and Ziemann, P. J. (2003). *On-line measurements of diesel nanoparticle composition and volatility*. Atmos Environ **37**(9-10): 1199-1210.

Saleh, R., Hennigan, C. J., McMeeking, G. R., Chuang, W. K., Robinson, E. S., Coe, H., Donahue, N. M. and Robinson, A. L. (2013). *Absorptivity of brown carbon in fresh and photo-chemically aged biomass-burning emissions*. Atmos Chem Phys **13**(15): 7683-7693.

Saleh, R., Robinson, E. S., Tkacik, D. S., Ahern, A. T., Liu, S., Aiken, A. C., Sullivan, R. C., Presto, A. A., Dubey, M. K., Yokelson, R. J., Donahue, N. M. and Robinson, A. L. (2014). *Brownness of organics in aerosols from biomass burning linked to their black carbon content*. Nat Geosci **7**(9): 647-650.

Salvi, S., Blomberg, A., Rudell, B., Kelly, F., Sandstrom, T., Holgate, S. T. and Frew, A. (1999). *Acute inflammatory responses in the airways and peripheral blood after short-term exposure to diesel exhaust in healthy human volunteers*. Am J Resp Crit Care **159**(3): 702-709.

Schauer, J. J., Kleeman, M. J., Cass, G. R. and Simoneit, B. R. T. (1999). *Measurement of emissions from air pollution sources. 2. C-1 through C-30 organic compounds from medium duty diesel trucks*. Environ Sci Technol **33**(10): 1578-1587.

Shiraiwa, M., Selzle, K. and Poschl, U. (2012). *Hazardous components and health effects of atmospheric aerosol particles: reactive oxygen species, soot, polycyclic aromatic compounds and allergenic proteins*. Free Radical Res **46**(8): 927-939.

Song, C., Na, K., Warren, B., Malloy, Q. and Cocker, D. R. (2007). *Impact of propene on secondary organic aerosol formation from m-xylene*. Environ Sci Technol **41**(20): 6990-6995.

Song, C., Na, K. S. and Cocker, D. R. (2005). *Impact of the hydrocarbon to NOx ratio on secondary organic aerosol formation*. Environ Sci Technol **39**(9): 3143-3149.

Tapanainen, M., Jalava, P. I., Maki-Paakkanen, J., Hakulinen, P., Happo, M. S., Lamberg, H., Ruusunen, J., Tissari, J., Nuutinen, K., Yli-Pirila, P., Hillamo, R., Salonen, R. O., Jokiniemi, J. and Hirvonen, M. R. (2011). *In vitro immunotoxic and genotoxic activities of particles emitted from two different small-scale wood combustion appliances*. Atmos Environ **45**(40): 7546-7554.

Tapanainen, M., Jalava, P. I., Maki-Paakkanen, J., Hakulinen, P., Lamberg, H., Ruusunen, J., Tissari, J., Jokiniemi, J. and Hirvonen, M. R. (2012). *Efficiency of log wood combustion affects the toxicological and chemical properties of emission particles*. Inhal Toxicol **24**(6): 343-355.

Textor, C., Schulz, M., Guibert, S., Kinne, S., Balkanski, Y., Bauer, S., Berntsen, T., Berglen, T., Boucher, O., Chin, M., Dentener, F., Diehl, T., Easter, R., Feichter, H., Fillmore, D., Ghan, S., Ginoux, P., Gong, S., Kristjansson, J. E., Krol, M., Lauer, A., Lamarque, J. F., Liu, X., Montanaro, V., Myhre, G., Penner, J., Pitari, G., Reddy, S., Seland, O., Stier, P., Takemura, T. and Tie, X. (2006). *Analysis and quantification of the diversities of aerosol life cycles within AeroCom*. Atmos Chem Phys **6**: 1777-1813.

Tkacik, D. S., Lambe, A. T., Jathar, S., Li, X., Presto, A. A., Zhao, Y., Blake, D., Meinardi, S., Jayne, J. T., Croteau, P. L. and Robinson, A. L. (2014). *Secondary Organic Aerosol Formation from in-Use Motor Vehicle Emissions Using a Potential Aerosol Mass Reactor*. Environ Sci Technol **48**(19): 11235-11242.

Torvela, T., Tissari, J., Sippula, O., Kaivosoja, T., Leskinen, J., Virén, A., Lähde, A. and Jokiniemi, J. (2014). *Effect of wood combustion conditions on the morphology of freshly emitted fine particles*. Atmos Environ **87**(0): 65-76.

Tsapakis, M. and Stephanou, E. G. (2003). *Collection of gas and particle semi-volatile organic compounds: use of an oxidant denuder to minimize polycyclic aromatic hydrocarbons degradation during high-volume air sampling*. Atmos Environ **37**(35): 4935-4944.

Tunved, P., Hansson, H. C., Kulmala, M., Aalto, P., Viisanen, Y., Karlsson, H., Kristensson, A., Swietlicki, E., Dal Maso, M., Strom, J. and Komppula, M. (2003). *One year boundary layer aerosol size distribution data from five nordic background stations*. Atmos Chem Phys **3**: 2183-2205.

Unosson, J., Blomberg, A., Sandstrom, T., Muala, A., Boman, C., Nystrom, R., Westerholm, R., Mills, N. L., Newby, D. E., Langrish, J. P. and Bosson, J. A. (2013). *Exposure to wood smoke increases arterial stiffness and decreases heart rate variability in humans*. Part Fibre Toxicol **10**.

Wang, H. (2011). *Formation of nascent soot and other condensed-phase materials in flames*. P Combust Inst **33**: 41-67.

Weilenmann, M., Favez, J. Y. and Alvarez, R. (2009). *Cold-start emissions of modern passenger cars at different low ambient temperatures and their evolution over vehicle legislation categories*. Atmos Environ **43**(15): 2419-2429.

Weitkamp, E. A., Sage, A. M., Pierce, J. R., Donahue, N. M. and Robinson, A. L. (2007). *Organic aerosol formation from photochemical oxidation of diesel exhaust in a smog chamber*. Environ Sci Technol **41**(20): 6969-6975.

Virtanen, A., Ristimäki, J., Marjamäki, M., Vaaraslahti, K., Keskinen, J. and Lappi, M., 2002: *Effective density of diesel exhaust particles as a function of size* (eds.)].

Wittbom, C., Eriksson, A. C., Rissler, J., Carlsson, J. E., Roldin, P., Nordin, E. Z., Nilsson, P. T., Swietlicki, E., Pagels, J. H. and Svenningsson, B. (2014). *Cloud droplet activity changes of soot aerosol upon smog chamber ageing*. Atmos Chem Phys **14**(18): 9831-9854.

Volkamer, R., Jimenez, J. L., San Martini, F., Dzepina, K., Zhang, Q., Salcedo, D., Molina, L. T., Worsnop, D. R. and Molina, M. J. (2006). *Secondary organic aerosol formation from anthropogenic air pollution: Rapid and higher than expected*. Geophys Res Lett **33**(17): -.

Yang, J. J., Gebremedhin, A. and Strand, M. (2013). *Characterization of Particles and Inorganic Vapors through High-Temperature Extraction in a Biomass-Fired Grate Boiler*. Energ Fuel **27**(10): 5915-5922.